Charles University in Prague
Faculty of Mathematics and Physics

DIPLOMA THESIS

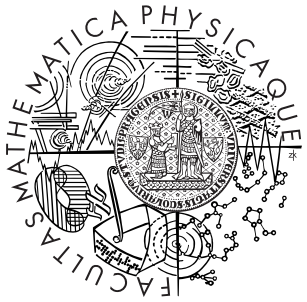

Artem Ryabov

Transcription of genetic information

Teoretický model přepisu genetické informace

Department of Macromolecular Physics

Supervisor: Doc. RNDr. Petr Chvosta, CSc.

Study programme: Physics, Physics of Condensed Matter and Materials

2010

I would like to express my gratitude to my supervisor Doc. RNDr. Petr Chvosta CSc. for his generous help with this thesis. I would also like to thank my family, friends and in particular my girlfriend Věra for their support and encouragement during my studies at the university.

I hereby declare that I have written the diploma thesis myself, using only cited sources. I agree with lending and distribution of the thesis.

Prague, April 15, 2010 Artem Ryabov

Contents

Název práce: Teoretický model přepisu genetické informace
Autor: Artem Ryabov
Katedra: Katedra makromolekulární fyziky
Vedoucí diplomové práce: Doc. RNDr. Petr Chvosta, CSc., Katedra makromolekulární fyziky
e-mail vedoucího: Petr.Chvosta@mff.cuni.cz
Abstrakt: V této práci je řešen jednodimenzionální model difúze částic ve vnějším časově proměnném silovém poli. Částice spolu interagují jen při srážkách, a to jako tuhé koule. Je nalezeno obecné exaktní řešení N-částicového problému. Jako konkrétní případ je studována difúze dvou částic na polopřímce s reflexní hranicí v počátku souřadnic, kdy na částice působí vnější harmonická sila. V důsledku interakce vzniká mezi částicemi efektivní odpudivé silové působení entropické povahy. Z daných důvodů se objevují nové efekty, které nejsou přítomny v případě difúze neinteragujících částic. Jedná se zejména o nárůst (pokles) práce vykonané na pravou (levou) částici. Stejnou vlastnost vykazují i střední polohy jednotlivých částic, produkce entropie jednotlivých částic a teplo odevzdané do tepelné lázně. Tyto veličiny jsou diskutovány v závislosti na parametrech modelu. Práce vykonaná na jednotlivou částici za jednu periodu vykazuje maximum jako funkce frekvence vnější síly. Produkce entropie navíc vykazuje maximum jako funkce teploty lázně a je symetrická vůči záměně teploty a frekvence.
Klíčová slova: kinetika difúze, termodynamika, exaktní řeseni, interakce

Title: Transcription of genetic information
Author: Artem Ryabov
Department: Department of Macromolecular Physics
Supervisor: Doc. RNDr. Petr Chvosta, CSc., Department of Macromolecular Physics
Supervisor's e-mail address: Petr.Chvosta@mff.cuni.cz
Abstract: We investigate a one-dimensional diffusive motion of a system of interacting Brownian particles driven by an external time-dependent force. We assume the hard-core interaction between the particles. We construct the exact general solution of the N-particle problem. Specifically, we assume the spatially restricted two-particles dynamics, and the harmonically oscillating driving force. The inter-particle interaction induces effective entropic forces and hence also new effects comparing to the corresponding model without the inter-particle interaction. Especially, we have found an increase (decrease) of the work done on the right (left) particle. Similar effects are exhibited by the one-particle mean position, the one-particle entropy production, and heat released to the bath. These characteristics have been discussed depending on the model parameters. Resonance-like maxima have been detected if we plot the work accepted by the individual particles as the function of the driving frequency. Similarly, the entropy production exhibits a maximum as the function of the bath temperature.
Keywords: single-file diffusion, exact solution, stochastic energetics, entropy

Chapter 1

Introduction and thesis organization

Stochastic dynamics of particles in a one-dimensional environment is both of great practical and theoretical interest. Due to the one-dimensionality of the problem, interactions among the particles play a crucial role and alter qualitative features of the particle dynamics. The type of interaction we deal with in this thesis is a so called *hard-core interaction*.

A survey of the scientific literature dealing with one-dimensional stochastic models of interacting particles led us into various parts of physics and mathematics. Similar models were formulated by different researchers independently of each other and solved using different theoretical methods. Chap. 2 presents the review of (from our point of view) fundamental articles on this topic. The *totally asymmetric exclusion process* (TASEP) is presented in Sec. 2.1. There follows a review of related models form probability theory, queue theory and statistical physics (Sec. 2.2). Sec. 2.3 is devoted to the discussion of a diffusion of Brownian particles which cannot pass each other – *the single-file diffusion*.

The afore-mentioned structure of Chap. 2 has been arranged in a chronological order. Initially we have been focused in the generalization of the TASEP. Due to this our first interest at the beginning of our work on the thesis, we have entitled it "Transcription of genetic information". However, we have rather solved the exclusion process in a continuous space (while the TASEP is a lattice model). Such a models belong to the class referred to as the single-file diffusion.

Although not many exact analytical results for the single-file diffusion of Brownian particles are known (see Sec. 2.3), this problem seems to be analytically tractable. The objectives of this thesis are to find out new exact analytical results in this field, to compare the diffusion dynamics of interacting particles with the diffusion dynamics of non-interacting particles and to study the effects of interaction occurred in thermody-

namic characteristics of the diffusion precess. To be specific, we construct the exact analytical solution for the problem of N hard-core interacting particles diffusing in an *arbitrary* (time-dependent) potential. As a particular example, we have studied in detail the diffusion of two hard-core interacting particles along the half-line with a reflecting boundary placed at the origin of coordinates. Particles were under the action of the time-oscillating force superimposed on the time-independent force. We calculate both the kinetic and the energetic characteristics of the emerging non-equilibrium isothermal process and discuss their dependence on the model parameters.

In Chap. 3 we present general concepts and define the model. In Sec. 3.1 we discuss a Smoluchowski diffusion equation and necessary related concepts. In Sec. 3.2 we formulate the hard-core interaction in terms of requirement posed on a probability current. Afterwards, we present basic concepts of stochastic energetics (Sec. 3.3) and entropy (Sec. 3.4).

The general solution is presented in Chap. 4. In Chap. 5 we discuss the properties of spatially restricted two-particle single-file diffusion process occurring in a half-space under the influence of a harmonically oscillating and space-homogeneous driving force. In Sec. 5.1 we numerically study a transient evolution of the probability densities. Then we derive exact analytical expressions for probability densities and particles mean positions in the time-asymptotic non-equilibrium regime. In this regime we analyse thermodynamic characteristics of the particles. Namely, in Sec. 5.2 we discuss the work done on the individual particles by an external agent (Subsec. 5.2.2), the heat released to the heat bath (Subsec. 5.2.3), the entropy and the entropy production (Subsec. 5.2.4) as the functions of model parameters. Finally, we summarize the main results and present the outstanding challenges (Chap. 6).

Chapter 2

Experimental impulses and theoretical approaches

2.1 Asymmetric simple exclusion process

Imagine a one-dimensional system where objects move with a preference in one direction and could not pass each other. It may represent any real system such as cars proceeding on a long narrow road, ribosomes travelling along the m-RNA or ions diffusing in a narrow channel. To advance the model towards the reality it is suitable to consider a finite system with *open* boundary condition, i.e., coupled to the particle reservoirs at either end. In terms of the traffic flow it we could study the road segment bounded by the traffic lights. Inside the cell, the ribosomes attach the m-RNA molecule at the one end (at the start codon), then they move along and they detach after the other end (the stop codon) is reached. Analogously, ions enter the narrow channel from the one side of the membrane and they leave it on the other side. The simplest model which captures the basics features of such a systems is *the totally asymmetric simple exclusion process* (TASEP).

The TASEP is defined as a stochastic process taking place on a discrete one-dimensional lattice with M sites. Each site is either occupied by one particle or empty. During the infinitesimal time interval dt each particle residing on sites $1, \dots, M-1$ has a probability dt of jumping to the next site on its right, provided that this site is empty. Furthermore the particle is added at the first site with a probability αdt if this site is empty and the particle is removed from the M-th site with probability βdt if this site is occupied [1, 2].

Up to our knowledge, the TASEP was first introduced in 1968 to describe the kinetics of protein synthesis [3, 4, 5]. Since then it further serves as the simple model for the

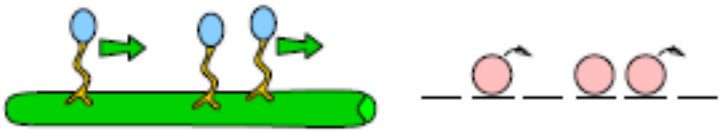

Figure 2.1: Kinesins attached to a microtubule that move in a preferred direction by extracting chemical energy from the environment. At a mesoscopic level, this can be modelled as a stochastic process in which particles hop along a one-dimensional lattice as shown. Figure was taken from [18].

transport across membranes [6], model for the traffic flow [7, 8, 9] exhibiting stable shocks analogous to traffic jams [10], transport in various biological systems [11]-[15] and has been widely discussed in the connection to the Kardar-Parisi-Zhang universality class [16]. The terminology of the simple exclusion process was first defined by Spitzer [17].

In addition to numerous applications, the TASEP has obtained the paradigmatic status as the exactly solvable model of non-equilibrium statistical physics in much the same way that the Ising model has become a paradigm for equilibrium critical phenomena. The TASEP exhibits interesting, purely non-equilibrium effects such as boundary-induced phase transitions, shock fronts and jamming [18].

The exact solution of the TASEP in the steady state has been obtained by Derrida et al. using a *matrix product ansatz* in [2]. After that the matrix product ansatz has become the important tool in the exploring non-equilibrium steady states in different systems. It was realized that it enables to solve quite a number of models (for a review see [18]).

Let us yet make a remark on the exact solution of the TASEP on the infinite line. It was obtained by Schütz in [19]. He showed that the transition probabilities between configurations of particles are given in terms of *determinant*.

2.2 Vicious walkers and Jackson networks

Excepted the TASEP and related exclusion processes, there exist several other exactly solved models of interacting random walking particles. For instance, Fisher in [50] have predicted quantitative features of the critical properties of wetting. For this purpose he introduced a conception of *vicious walkers*. Abhorrent to their horrible name, the vicious walkers were simply symmetrically random walking particles on the one-dimensional

integer lattice with the requirement that whenever two vicious walkers occur at the same site, they immediately kill each other. On the other words, in such a random walk, two particles annihilate whenever they collide. Fisher in his work [50] has showed that the partition function[1] for this model in free boundary conditions can be expressed as a determinant.

Fisher's model is in fact a particular example of so called *non-colliding Markov processes*. These processes are canonical examples of stochastic processes with a determinantal transition kernel, given by the Karlin-McGregor formula [44]. The connection between this processes and Schütz kernel [19] for TASEP on a line has been recently realized and explained by Dieker and Warren in [47].

Again, Dieker and Warren in their other paper [48] have shown another interesting connection. Namely, between queue theory an the TASEP. More precisely, between the series N-node Jackson networks and the Schütz kernel [19]. Series Jackson networks were exactly solved by Massey [45] in terms of lattice Bessel functions. After finding the general solution, Massey together with Baccelli have considered a two-node Jackson network in [46]. An alternative approach to this problem was developed by Böhm in [49]. He used rather probabilistic arguments and expressed corresponding probabilities in terms of the sum of determinants.

2.3 Single-file diffusion of Brownian particles

One-dimensional diffusion of hard-core interacting particles (i.e., the diffusion of the particles which are not able to pass each other) is known as the *single-file diffusion* (SFD). The concept of SFD was first introduced by Hodgkin[2] and Keynes[3] in biophysics, when they tried to explain the transport of water and ions through the molecular-sized channels in membranes [20]. Since then, numerous examples of SFD in biological, chemical, and physical processes were studied, e.g. transport of adsorbate molecules through zeolites with a one-dimensional channel system [21, 22, 23], geometrically constrained nano-sized particles in nano-sized pores [24], migration of adsorbed molecules on surfaces [25], diffusion in nanotubes [30, 31], diffusion of colloids in one-dimensional channels (see Fig. 2.2) [26, 28, 29], a carrier migration in polymers and superionic conductors [32].

While the collective motion of particles in such a system proceeds just like that of independent particles, the dynamics of individual (also called *tagged particle* or *tracer*)

[1] In this context the partition function counts the number of ways in which N random walking particles, can depart certain initial sites and arrive at given new sites.

[2] The 1963 Nobel Prize winner in Physiology or Medicine.

[3] One perhaps interesting remark: R. D. Keynes is the great-grandson of Charles Darwin.

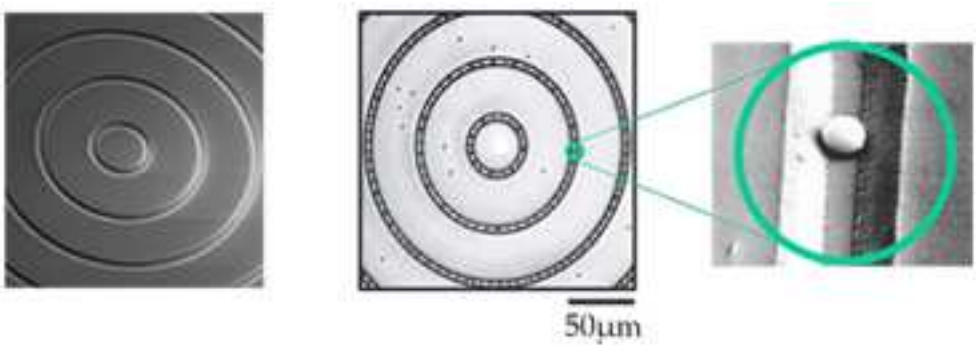

Figure 2.2: An illustration of the experimentally studied single-file system. The left picture is a scanning electron microscope image of the one-dimensional trenches fabricated on the photoresist polymer film by photolithography. The middle picture shows an optical microscope image of three concentric circular channels with colloidal particles confined in them (the small black objects inside the channels) [26]. This figure was taken from [27].

particles is considerably different [34, 35, 36]. Theoretical description of SFD was first introduced by Harris in 1965. In his pioneering study [33] he showed that the mean square displacement (MSD) of a tagged particle growth with time as $t^{1/2}$ (in contrast to non-interacting particles, which MSD growth as t). This result was subsequently reestablished by various others using different methods. For a comprehensive review of articles dealing with the derivation of $t^{1/2}$ law of MSD in single-file systems see an introduction in [37]. In the following we rather concentrate on a review of known exact analytical solutions of the single-file diffusion of Brownian particles. By the term "exact solution" we will understand the exact solution of the underlying diffusion equation, i.e., the probability density of the positions of particles.

The first exact solution for an arbitrary number N of identical particles diffusing along the infinite line has been obtained by Rödenbeck et al. in [34] via the reflection principle. The different derivation of the probability density for the same problem is presented in [38]. The exact solution on the finite interval has been found in [37] through the Bethe ansatz (for an introduction to this technique see e.g. a review [39] and references herein). The exact solution for particles with different diffusion constants has been obtained in [40] but only for $N = 2$. Another remarkable exact result for $N = 2$ has been derived in [41]. Here authors have found the exact solution for two particles interacting by a finite potential. As the height of the interaction potential tends to infinity, the limit of hard-core interacting particles is obtained. Unfortunately both results in [40] and [41] were obtained by the transformation of the coordinates into the

center-of-mass coordinate system, hence it cannot be generalized for an arbitrary N. Recently have been made the attempts to obtain the exact solution in a presence of the external force-field. Using a so called "Jepsen line", the probability density for the center particle was obtain in the limit of an infinite system with constant particle density in [42, 43]. Up to our knowledge, so far, no exact solution for the single-file diffusion of N particles diffusing under the action of the external force has been derived.

Chapter 3

Model setting

3.1 Smoluchowski diffusion equation

We are interested in the dynamics of over-damped Brownian particles diffusing in an external potential in one dimension. Considering first the single-particle case, the dynamics can be described by the Langevin equation

$$\Gamma \frac{\mathrm{d}}{\mathrm{d}t}\mathsf{X}(t) = F_L(t) + F(\mathsf{X}(t), t) \ , \tag{3.1}$$

where the random variable $\mathsf{X}(t)$ represents the position of the particle, $F(\mathsf{X}(t), t)$ is the time-dependent *external* force, $F_L(t)$ is the δ-correlated Langevin force and Γ equals the particle mass times the viscous friction coefficient $\Gamma = m\gamma$. In this over-damped regime, the time-evolution equation for a probability density of the position of the Brownian particle is the *Smoluchowski equation*[1]

$$\frac{\partial}{\partial t} p(x; t \,|\, y; t_0) = \left\{ -\frac{\partial}{\partial x} v(x,t) + D \frac{\partial^2}{\partial x^2} \right\} p(x; t \,|\, y; t_0) \ . \tag{3.2}$$

The first term on the right-hand side, the so called "drift term", or "convection term", describes the time change of the probability density $p(x; t \,|\, y; t_0)$ caused by the external force. The *drift velocity* $v(x,t)$ is defined as

$$v(x,t) \equiv \frac{1}{\Gamma} F(x,t) = -\frac{1}{\Gamma} \frac{\partial}{\partial x} \phi(x,t) \ , \tag{3.3}$$

[1] For a detailed discussion of the over-damped regime and derivation of Eq. (3.2) from the Langevin equation, see [51], [52] or [53].

where $\phi(x,t)$ denotes the time-dependent potential of the force $F(x,t)$. The second term on the right-hand of Eq. (3.2), the so called "diffusion term" or "fluctuation term", describes the spreading of the particle position due to the thermal force. The *diffusion constant* D is related to the temperature of the environment T, mass of the Brownian particle m and the damping coefficient γ. We have [51]

$$D = \frac{k_B T}{m\gamma} \ . \tag{3.4}$$

The probability density $p(x;t\,|\,y;t_0)$ multiplied by an infinitesimally small interval of the width $\mathrm{d}x$ yields the probability of finding the particle at the time t inside the interval $(x, x+\mathrm{d}x)$, provided that at the time t_0 ($t_0 \leq t$) the particle was located at the position y. In symbols we have

$$p(x;t\,|\,y;t_0)\,\mathrm{d}x = \mathrm{Prob}\{\mathsf{X}(t) \in (x, x+\mathrm{d}x)\,|\,\mathsf{X}(t_0) = y\} \ , \tag{3.5}$$

$$p(x;t_0\,|\,y;t_0) = \delta(x-y) \ . \tag{3.6}$$

Here $\delta(x)$ denotes the Dirac delta function at $x = 0$. The last equation sets the initial condition for the linear partial differential equation (3.2). The boundary conditions can be included through the potential $\phi(x,t)$ and they will be specified below.

The Smoluchowski equation (3.2) can be written in the form of a continuity equation for the probability density

$$\frac{\partial}{\partial t} p(x;t\,|\,y;t_0) = -\frac{\partial}{\partial x} J(x;t\,|\,y;t_0) \ , \tag{3.7}$$

where

$$J(x;t\,|\,y;t_0) = \left\{ v(x,t) - D\frac{\partial}{\partial x} \right\} p(x;t\,|\,y;t_0) \tag{3.8}$$

is the *probability current*.

Up to now, we have been discussing the diffusion dynamics of just one isolated Brownian particle. Let us now turn to the case of N over-damped Brownian particles labelled from 1 to N. We denote the probability density of their positions as $p^{(N)}(x_1, \ldots, x_N; t\,|\,y_1, \ldots, y_N; t_0)$. An interpretation of this probability density is similar to Eq. (3.5). If we multiply this density by the product $\mathrm{d}x_1, \ldots, \mathrm{d}x_N$, then the resulting expression is the probability of the simultaneous occurrence of the particle labelled by 1 inside the interval $(x_1, x_1+\mathrm{d}x_1)$, particle labelled by 2 inside the interval $(x_2, x_2+\mathrm{d}x_2)$, ..., particle labelled by N inside the interval $(x_N, x_N+\mathrm{d}x_N)$ at the time t, provided that at the initial time t_0 ($t_0 \leq t$), these particles were located at positions $y_1, y_2, \ldots, y_N$,

respectively. Further, we assume that all N particles are identical (i.e., they possess the same masses m, the damping coefficients γ and the effects of the external force on each particle are described by the potential $\phi(x_i, t)$, $i = 1, \dots, N$ same for all particles). Then the Smoluchowski equation reads

$$\frac{\partial}{\partial t} p^{(N)}(x_1, \dots, x_N; t \,|\, y_1, \dots, y_N; t_0) =$$
$$= \sum_{j=1}^{N} \left\{ -\frac{\partial}{\partial x_j} \left[v(x_j, t) + v_j^{\mathrm{int}}(x_1, \dots, x_N, t) \right] + D \frac{\partial^2}{\partial x_j^2} \right\} p^{(N)}(x_1, \dots, x_N; t \,|\, y_1, \dots, y_N; t_0) \tag{3.9}$$

with the initial condition

$$p^{(N)}(x_1, \dots, x_N; t_0 \,|\, y_1, \dots, y_N; t_0) = \delta(x_1 - y_1) \dots \delta(x_N - y_N) \ . \tag{3.10}$$

The only additional terms in Eq. (3.9) which have not appeared in Eq. (3.2) are $v_j^{\mathrm{int}}(x_1, \dots, x_N, t)$, $j = 1, \dots, N$. For a given j this term involves the force (divided by Γ) exerted on the j-th Brownian particle by other Brownian particles. Hence it describes an interaction between the particles. In the rest of the thesis we will exclusively deal with the so called *hard-core interaction*.

3.2 Hard-core interaction

In order to incorporate the simplest inter-particle interaction, the particles can be represented as rods of the length l. The hard-core interaction in such system means that the space occupied by one rod is inaccessible to the neighbouring rods. Theoretically the diffusion of hard rods can be mapped exactly onto the diffusion of *point particles* (particles with the linear size $l = 0$) by the simple rescaling of space variables (see e.g. [37]). Hence without the lost of generality all further considerations will be done for systems of point particles.

3.2.1 Two particles

Consider two identical hard-core interacting particles, each with the diffusion constant D, diffusing in the potential $\phi(x, t)$. Due to the hard-core interaction, *particles cannot pass each other*. Therefore the ordering of the particles is preserved during the evolution, i.e., starting with $y_1 < y_2$, we have

$$-\infty < \mathsf{X}_1(t) < \mathsf{X}_2(t) < +\infty \tag{3.11}$$

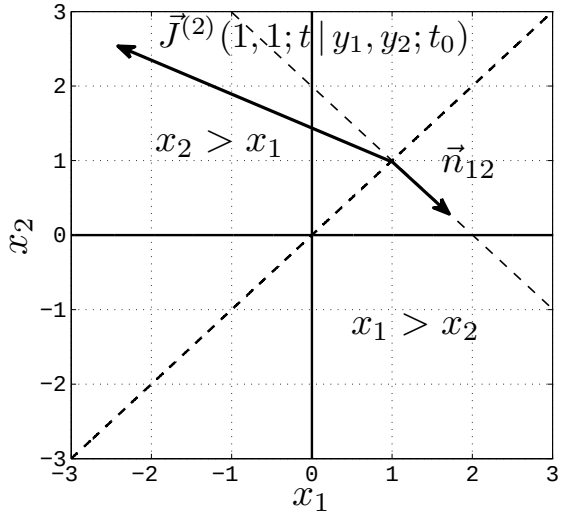

Figure 3.1: Graphical representation of the restriction (3.11). The probability current in the direction $\vec{n}_{12}$ at the line $x_1 = x_2$ must be zero.

for any t. We can then call the particle with the coordinate $\mathsf{X}_1(t)$ ($\mathsf{X}_2(t)$) as the left (right) one.

Note that for $x_1 \neq x_2$ both particles diffuse as non-interacting particles. This enables us to describe the diffusion of two identical hard-core interacting particles in one dimension as the diffusion of one "representative" particle in the *half-plane* $x_2 > x_1$ (see Fig. 3.1)[2]. This picture corresponds to the condition that the probability current in the direction perpendicular to the line $x_1 = x_2$ vanishes at this line. Otherwise the dynamics inside the half-plane $x_1 < x_2$ is controlled by the Smoluchowski equation

$$\frac{\partial}{\partial t} p^{(2)}(x_1, x_2; t \,|\, y_1, y_2; t_0) = -\sum_{j=1}^{2} \frac{\partial}{\partial x_j} J_j^{(2)}(x_1, x_2; t \,|\, y_1, y_2; t_0) \;, \tag{3.12}$$

where

$$J_j^{(2)}(x_1, x_2; t \,|\, y_1, y_2; t_0) = \left\{ v(x_j, t) - D \frac{\partial}{\partial x_j} \right\} p^{(2)}(x_1, x_2; t \,|\, y_1, y_2; t_0) \tag{3.13}$$

is the j-th component of the probability current. The current in the direction perpendicular to the line $x_1 = x_2$ is obtained by a scalar multiplication of the current vector

[2]The only purpose of the mapping is to elucidate conditions further imposed on the probability current.

$\vec{J}^{(2)} = (J_1^{(2)}, J_2^{(2)})$ with the normal vector $\vec{n}_{12} = (1, -1)/\sqrt{2}$. The result must be zero at the line $x_1 = x_2$, i.e., we require that

$$\vec{J}^{(2)}(x_1, x_2; t \,|\, y_1, y_2; t_0) \cdot \vec{n}_{12}\Big|_{x_1=x_2} = 0 \ . \tag{3.14}$$

After the substitution for the current $\vec{J}^{(2)}$ from Eq. (3.13), the requirement (3.14) assumes the form

$$\left(\frac{\partial}{\partial x_2} - \frac{\partial}{\partial x_1}\right) p^{(2)}(x_1, x_2; t \,|\, y_1, y_2; t_0)\Big|_{x_1=x_2} = 0 \ . \tag{3.15}$$

This condition implies that the representative particle cannot cross the line $x_1 = x_2$. Returning to the original picture, *the two hard-core interacting particles in one dimension will never cross each other.*

Let us summarize the results of this Subsection. In order to obtain the probability density $p^{(2)}(x_1, x_2, t \,|\, y_1, y_2, t_0)$ for two identical hard-core interacting Brownian particles, one has to solve the Smoluchowski equation (3.12) (i.e., the equation *without interaction*) with the *non-crossing boundary condition* (3.15) and the initial condition

$$p^{(2)}(x_1, x_2; t_0 \,|\, y_1, y_2; t_0) = \delta(x_1 - y_1)\delta(x_2 - y_2) \ . \tag{3.16}$$

All these considerations can be straightforwardly generalized to the N-particle case. In the next Subsection we will formulate the *central general objective* of the thesis.

3.2.2 N particles

Consider N identical hard-core interacting particles, each with the diffusion constant D, diffusing along the line in the external potential $\phi(x, t)$. If we label the particles $1, \ldots, N$ from left to right, then for all times the order of particles has to be conserved, i.e., inequality

$$-\infty < \mathsf{X}_1(t) < \mathsf{X}_2(t) < \ldots < \mathsf{X}_N(t) < +\infty \tag{3.17}$$

holds at any instant ($\mathsf{X}_i(t)$ is the coordinate of the i-th particle). We are to solve the Smoluchowski equation

$$\begin{aligned} &\frac{\partial}{\partial t} p^{(N)}(x_1, \ldots, x_N; t \,|\, y_1, \ldots, y_N; t_0) = \\ &= \sum_{j=1}^{N} \left\{ -\frac{\partial}{\partial x_j} v(x_j, t) + D \frac{\partial^2}{\partial x_j^2} \right\} p^{(N)}(x_1, \ldots, x_N; t \,|\, y_1, \ldots, y_N; t_0) \end{aligned} \tag{3.18}$$

for the N-particle probability density $p^{(N)}(x_1, \ldots, x_N; t \,|\, y_1, \ldots, y_N; t_0)$ with the initial condition

$$p^{(N)}(x_1, \ldots, x_N; t_0 \,|\, y_1, \ldots, y_N; t_0) = \delta(x_1 - y_1) \ldots \delta(x_N - y_N) \ , \tag{3.19}$$

where where $y_1 < \ldots < y_N$. The probability density has to satisfy the *non-crossing boundary conditions*

$$\left(\frac{\partial}{\partial x_{j+1}} - \frac{\partial}{\partial x_j} \right) p^{(N)}(x_1, \ldots, x_N; t \,|\, y_1, \ldots, y_N; t_0) \Big|_{x_{j+1} = x_j} = 0 \ , \tag{3.20}$$

where $j = 1, \ldots, N-1$.

3.3 Stochastic energetics

Time dependence of the driving force affords us an opportunity to study the *energetics* of the diffusion process. In this Subsection we define an internal energy of one diffusing particle, work done on one particle by an external agent and heat dissipated to the heat bath.

The arguments of stochastic energetics [54] are based on the Langevin equation. The position of the particle is represented by the random variable $\mathsf{X}(t)$. If the particle occurs at an arbitrary fixed instant at the position $\mathsf{X}(t)$, it has the potential energy $\phi(\mathsf{X}(t), t)$. From this perspective, having solved the Smoluchowski equation, we know the probability density of a random variable $\mathsf{X}(t)$. The average internal energy is then the probabilistic mean value of the random variable $\phi(\mathsf{X}(t), t)$, i.e., we have

$$E(t|\, y; t_0) = \langle \phi(\mathsf{X}(t), t) \rangle = \int_{-\infty}^{+\infty} \mathrm{d}x \, \phi(x, t) \, p(x; t \,|\, y; t_0) \tag{3.21}$$

The applied methods of stochastic energetics incorporate also the separate calculation of both the heat and the work. Generally speaking the heat ($\equiv$ the dissipated energy) arises if and only if the particle moves, i.e. it is inevitable connected with the probability density current. More precisely, the heat released to the heat bath during the time interval $[t_0, t]$ is given as

$$Q(t \,|\, y; t_0) = \int_{t_0}^{t} \mathrm{d}t' \int_{-\infty}^{+\infty} \mathrm{d}x \left[-\frac{\partial}{\partial x} \phi(x, t') \right] J(x; t' \,|\, y; t_0) \ . \tag{3.22}$$

On the other hand, the external agent does work on the system by lifting the potential $\phi(x, t)$, while the position of the particle is virtually fixed. Averaging over the possible

positions, the work done by the external force during the interval $[t_0, t]$ reads

$$W(t \,|\, y; t_0) = \int_{t_0}^{t} \mathrm{d}t' \int_{-\infty}^{+\infty} \mathrm{d}x \left[\frac{\partial}{\partial t'} \phi(x, t') \right] p(x; t' \,|\, y; t_0) \ . \tag{3.23}$$

3.4 Entropy

Entropy increase of the heat bath during the time interval $[t_0, t]$, say $S(t \,|\, y; t_0)$, equals to heat released to the bath during this interval, divided by the temperature of the heat bath. For one diffusing particle the heat is given by Eq. (3.22), hence we have

$$S(t \,|\, y; t_0) = \frac{Q(t \,|\, y; t_0)}{T} \ . \tag{3.24}$$

We define an instantaneous entropy of the diffusing particle $H(t \,|\, y; t_0)$ as follows,

$$H(t \,|\, y; t_0) = - k_{\mathrm{B}} \int_{-\infty}^{+\infty} \mathrm{d}x \, p(x; t \,|\, y; t_0) \log p(x; t \,|\, y; t_0) \ . \tag{3.25}$$

Its absolute value possesses no physical meaning ($H(t \,|\, y; t_0)$ could be even negative)[57]. The difference $H(t^* \,|\, y; t_0) - H(t^{**} \,|\, y; t_0)$ yields the difference between the particle's entropy at the time t^* and its entropy at the time t^{**}.

Finally, let us introduce the Kullback-Leibler entropy [55], also known as the relative entropy or the Kullback-Leibler divergence. The Kullback-Leibler entropy could be understood as a measure of difference between two random variables. Its definition reads

$$K[p, q] = \int_{-\infty}^{+\infty} \mathrm{d}x \, p(x; t \,|\, y; t_0) \log \left[\frac{p(x; t \,|\, y; t_0)}{q(x; t \,|\, y; t_0)} \right] \ , \tag{3.26}$$

where $p(x; t \,|\, y; t_0)$ and $q(x; t \,|\, y; t_0)$ are the probability densities of two random variables that we are comparing. It even exhibits some property of the distance characteristics, that of being positive and that of being equal to zero if and only if $p(x; t \,|\, y; t_0) = q(x; t \,|\, y; t_0)$. However, it is not a true distance between distributions since it is not symmetric ($K[p, q] \neq K[q, p]$) and does not satisfy the triangle inequality [56].

Chapter 4

General solution

In this Chapter we state a general theorem concerning the form of the solution of the Smoluchowski equation for N hard-core interacting particles. The solution is very important in the following Chapter. It enables us to construct the probability density function corresponding to the *many particle problem with a hard-core interaction* from the simpler elements which are *one-particle probability density functions.*[1]

Theorem 4.1. *Let the single-particle probability density* $p(x;t\,|\,y;t_0)$ *be the solution of the Smoluchowski equation*

$$\frac{\partial}{\partial t}p(x;t\,|\,y;t_0) = \left\{-\frac{\partial}{\partial x}v(x,t) + D\frac{\partial^2}{\partial x^2}\right\}p(x;t\,|\,y;t_0) \tag{4.1}$$

with the initial condition

$$p(x;t_0\,|\,y;t_0) = \delta(x-y)\ . \tag{4.2}$$

Then, the probability density function, which is the solution of the problem stated in Subsec. 3.2.2 *reads*

$$\begin{aligned} &p^{(N)}(x_1,\ldots,x_N;t\,|\,y_1,\ldots,y_N;t_0) = \\ &\qquad = \sum_{\pi} p(x_1;t\,|\,\pi(y_1);t_0)\,p(x_2;t\,|\,\pi(y_2);t_0)\ldots p(x_N;t\,|\,\pi(y_N);t_0)\ , \end{aligned} \tag{4.3}$$

where the summation is taken over all $N!$ *permutations* π *of the set* $\{y_1,\ldots,y_N\}$ *of initial conditions, where* $y_1 < y_2 < \ldots < y_N$.

For a convenience of the reader we now present the proof for a particular case, namely for $N = 2$. This proof includes also a discussion of main general properties of the solution (4.3). A proof for an arbitrary N is a straightforward generalization of the following.

[1] Similar theorem but for the diffusion on *infinite* line and *without* external force was used in [38].

Proof: Assuming $N = 2$, we have to show that the solution of the problem as formulated in Subsec. 3.2.1 has the form

$$\begin{aligned} p^{(2)}(x_1, x_2; t \,|\, y_1, y_2; t_0) = & \, p(x_1; t \,|\, y_1; t_0) p(x_2; t \,|\, y_2; t_0) + \\ & + p(x_1; t \,|\, y_2; t_0) p(x_2; t \,|\, y_1; t_0) \end{aligned} \tag{4.4}$$

within the phase space

$$\mathcal{R}_2 : -\infty < x_1 < x_2 < +\infty \ ,$$

and is *identically equal to zero elsewhere* (cf. Fig. 3.1).

Differently speaking, we are to demonstrate that the function (4.4) satisfies the Smoluchowski equation (3.12) with the initial condition (3.16), and non-crossing boundary conditions (3.15) provided that the probability density $p(x; t \,|\, y; t_0)$ solves Eq. (4.1) with the initial condition (4.2).

We shall first insert the function (4.4) into the dynamical equation (3.12). After rearranging the terms, we have

$$\begin{aligned} 0 = & \, p(x_1; t \,|\, y_1; t_0) \left\{ \frac{\partial}{\partial t} + \frac{\partial}{\partial x_2} v(x_2, t) - D \frac{\partial^2}{\partial x_2^2} \right\} p(x_2; t \,|\, y_2; t_0) + \\ & + p(x_2; t \,|\, y_2; t_0) \left\{ \frac{\partial}{\partial t} + \frac{\partial}{\partial x_1} v(x_1, t) - D \frac{\partial^2}{\partial x_1^2} \right\} p(x_1; t \,|\, y_1; t_0) + \\ & + p(x_1; t \,|\, y_2; t_0) \left\{ \frac{\partial}{\partial t} + \frac{\partial}{\partial x_2} v(x_2, t) - D \frac{\partial^2}{\partial x_2^2} \right\} p(x_2; t \,|\, y_1; t_0) + \\ & + p(x_2; t \,|\, y_1; t_0) \left\{ \frac{\partial}{\partial t} + \frac{\partial}{\partial x_1} v(x_1, t) - D \frac{\partial^2}{\partial x_1^2} \right\} p(x_1; t \,|\, y_2; t_0) \ . \end{aligned} \tag{4.5}$$

However, according to assumptions the densities $p(x; t \,|\, y; t_0)$ satisfy the Smoluchowski equation (4.1). Hence the individual terms on the right-hand side of Eq. (4.5) vanish. Therefore, the function (4.4) satisfies the Smoluchowski equation (3.12).

Now we check the validity of the non-crossing boundary conditions. After the substitution of the function (4.4) into Eq. (3.15) we obtain

$$\begin{aligned} & \left\{ p(x_1; t \,|\, y_1; t_0) \frac{\partial}{\partial x_2} p(x_2; t \,|\, y_2; t_0) - p(x_2; t \,|\, y_1; t_0) \frac{\partial}{\partial x_1} p(x_1; t \,|\, y_2; t_0) + \right. \\ & \left. + p(x_1; t \,|\, y_2; t_0) \frac{\partial}{\partial x_2} p(x_2; t \,|\, y_1; t_0) - p(x_2; t \,|\, y_2; t_0) \frac{\partial}{\partial x_1} p(x_1; t \,|\, y_1; t_0) \right\} \Bigg|_{x_1 = x_2} = 0 \ . \end{aligned} \tag{4.6}$$

After applying $x_1 = x_2$ in the curly brackets, the first two terms (the last two terms) sum up to zero. Therefore the function (4.4) actually satisfies the non-crossing boundary conditions.

In the last step we have to show that the density (4.4) fulfils the initial condition (3.16) when $t \to t_0$. Using the unit-step function $\theta(x)$

$$\theta(x) = \begin{cases} 1 & \text{for } x > 0 \ , \\ 0 & \text{for } x \leq 0 \ , \end{cases} \tag{4.7}$$

the density (4.4) can written in the form

$$\begin{aligned} p^{(2)}(x_1, x_2; t \,|\, y_1, y_2; t_0) = \theta(x_2 - x_1) \, [p(x_1; t \,|\, y_1; t_0) p(x_2; t \,|\, y_2; t_0) + \\ + \, p(x_1; t \,|\, y_2; t_0) p(x_2; t \,|\, y_1; t_0)] \ . \end{aligned} \tag{4.8}$$

valid for *any* $x_1, x_2 \in (-\infty, +\infty)$. If we take the limit $t \to t_0$, we obtain

$$\begin{aligned} \lim_{t \to t_0} p^{(2)}(x_1, x_2; t \,|\, y_1, y_2; t_0) = \theta(x_2 - x_1) \delta(x_1 - y_1) \delta(x_2 - y_2) + \\ + \, \theta(x_2 - x_1) \delta(x_1 - y_2) \delta(x_2 - y_1) \ . \end{aligned} \tag{4.9}$$

However, because of the assumed initial ordering $y_1 < y_2$, the second term vanishes and we get

$$\lim_{t \to t_0} p^{(2)}(x_1, x_2; t \,|\, y_1, y_2; t_0) = \delta(x_1 - y_1) \delta(x_2 - y_2) \ . \tag{4.10}$$

Chapter 5

Explicit analysis of two particle problem

Consider the single-file diffusion of two identical over-damped Brownian particles, each with the diffusion constant D, diffusing in the time-dependent potential

$$\phi(x_i,t) = \begin{cases} -\,x_i\,F(t) & \text{for} \quad x_i > 0\ , \\ \\ +\infty & \text{for} \quad x_i < 0\ , \quad i = 1,2\ . \end{cases} \tag{5.1}$$

This means that each particle is acted upon by the same space-homogeneous and time-dependent force $F(t)$[1]. Assuming again $y_1 < y_2$, we shall call the particle with the coordinate $\mathsf{X}_1(t)$ ($\mathsf{X}_2(t)$) the *left* (*right*) one. Our primarily interest is to investigate the response of this system to the *time-oscillating* external force. The external driving force to be discussed in the rest of the thesis will consist of two components

$$F(t) = F_0 + F_1 \sin(\omega t)\ . \tag{5.2}$$

The time-independent component F_0 will push the particles to the left against the reflecting boundary at the origin (if $F_0 < 0$), or to the right (if $F_0 > 0$). The time-dependent component $F_1 \sin(\omega t)$ harmonically oscillates with the angular frequency ω.

We shall focus on the dynamical consequences of the interaction of the particles. Therefore we contrast the dynamics of the system of the two interacting particles against the standard model, in witch the interaction is switched off. In the standard model with the two non-interacting particles, the analysis trivially follows from the diffusion

[1] In other words, we consider a diffusion on the half line $x \in (0, +\infty)$ with a reflecting boundary at the origin.

problem concerning just one particle. In this context we refer to it as to the *single-diffusing particle*.

Further we will always take $\Gamma = 1.0\,\mathrm{kg\,s^{-1}}$. However, the analytical results will be mostly expressed in terms of the *drift velocity* $v(t) = F(t)/\Gamma$ (cf. Eq. (3.3)) and its components. We have

$$v(t) = v_0 + v_1 \sin(\omega t) \ , \tag{5.3}$$

with $v_0 = F_0/\Gamma$ and $v_1 = F_1/\Gamma$. We remind that $\Gamma = 1/(m\gamma)$, where m is the mass the particle, and γ is the viscous friction coefficient.

On the whole our model includes four parameters F_0, F_1, ω, and D. The parameters F_0, F_1, ω are related to the driving force and the parameter D is proportional to the bath temperature T. Notice that the hard-core interaction among particles acts as a purely geometric restriction. As such, it is not described by any "parameter of interaction".

5.1 Dynamics

5.1.1 Probability density function

The joint conditional probability density function of positions of two interacting particles diffusing in potential (5.1), say $p^{(2)}(x_1, x_2, t \,|\, y_1, y_2)$, may be constructed from one-particle conditional probability density functions as (cf. Theorem 4.1 in Chap. 4)

$$\begin{aligned} p^{(2)}(x_1, x_2; t \,|\, y_1, y_2) = \theta(x_2 - x_1) \, [u(x_1; t \,|\, y_1) \, u(x_2; t \,|\, y_2) + \\ + \, u(x_1; t \,|\, y_2) \, u(x_2; t \,|\, y_1)] \ , \end{aligned} \tag{5.4}$$

where $x_1, x_2 \in (0, +\infty)$ are particles' positions at time t, y_1 and y_2 are their initial positions, i.e., positions at the time zero, Finally, two remarks concerning the designation are in order. First, the initial condition is always taken at the time $t_0 = 0$ and we skip out the variable t_0. Secondly, the single-particle solution valid specially for the potential (5.1) will be designated as $u(x; t \,|\, y)$. In the present context, this density plays the same role as the density $p(x; t \,|\, y; t_0)$ in the preceding Chapter 4.

Hence, our first task is to find an expression for the function $u(x; t \,|\, y)$. This single-particle problem has been previously treated by P. Chvosta et al. in [58] and [59]. In [58] an integral equation for the function $u(x; t \,|\, y)$ has been derived. Subsequently in [59] an exact time-asymptotic expression for this function was given. Below, we will partially follow the analysis presented in [58] and [59].

In order to obtain the single-particle solution $u(x; t \,|\, y)$, we first consider the unrestricted diffusion of the particle in the field of a spatially-homogeneous and time-dependent force (i.e., drift velocity $v(t)$ now arbitrary depends on time, but not on the

space variable). The time-evolution of the probability density for the position of the diffusing particle reads [60, 61, 62]

$$g(x;t\,|\,y;t') = \frac{1}{\sqrt{\pi}}\,\frac{1}{\sqrt{4D(t-t')}}\exp\left\{-\frac{1}{4D(t-t')}\left[x-y-\int_{t'}^{t}\mathrm{d}t''\,v(t'')\right]^2\right\}\ . \quad (5.5)$$

We now assume that the particle is initially fully localised at a fixed point $y > 0$. The probability density function which corresponds to the problem with the reflecting boundary at the origin of coordinates, $u(x;t\,|\,y)$, can be constructed in two steps (cf. the detailed derivation in [58]). First, one has to solve the Volterra integral equation of the first kind

$$D\int_0^t \mathrm{d}t'\,g(0;t\,|\,0;t')\,u(0;t'\,|\,y) = \int_{-\infty}^{0}\mathrm{d}x\,g(x;t\,|\,y;0)\ . \quad (5.6)$$

Here both the kernel and the right hand side follow directly from Eq. (5.5). The integral equation should be solved for the unknown function $u(0;t\,|\,y)$ which represents, as the designation suggests, the time evolution of the probability density for the restricted diffusion at the reflecting boundary. Therefore, the solution must be a non-negative function of time. In the second step, the solution of the integral equation (5.6) yields the full space-resolved density $u(x;t\,|\,y)$. As a matter of fact, having obtained the probability density at the boundary, the final space-resolved solution emerges after performing just one additional quadrature. In [58] the formula

$$u(x;t\,|\,y) = g(x;t\,|\,y;0) - D\int_0^t \mathrm{d}t'\,\frac{\partial}{\partial x}g(x;t\,|\,0;t')\,u(0;t'\,|\,y) \quad (5.7)$$

has been proved. It is easy to see that the resulting function is properly normalized, i.e., we have $\int_0^{+\infty}\mathrm{d}x\,u(x;t\,|\,y) = 1$ for any $t \geq 0$ and for any fixed initial position $y > 0$.

Inserting formula (5.7) into Eq. (5.4) completes the derivation of the two-particle probability density $p^{(2)}(x_1,x_2;t\,|\,y_1,y_2)$. After integrating this function over the coordinate x_1 of the left particle we arrive at the (marginal) probability density describing the dynamics of the right particle. Similarly, the probability density of the left particle emerges from the formula

$$p_{\mathrm{L}}(x;t\,|\,y_1,y_2) \equiv \int_0^{+\infty}\mathrm{d}x_2\,p^{(2)}(x,x_2;t\,|\,y_1,y_2)\ , \quad (5.8)$$

$$p_{\mathrm{R}}(x;t\,|\,y_1,y_2) \equiv \int_0^{+\infty}\mathrm{d}x_1\,p^{(2)}(x_1,x;t\,|\,y_1,y_2)\ . \quad (5.9)$$

Notice that both marginal densities depend on the initial positions of the *both* particles. Understandably, this is a direct consequence of the the interaction among the particles.

We now derive an important identity concerning the sum of marginal densities (5.8) and (5.9). Carrying out the required integrations in (5.4) and using the normalization condition for $u(x;t\,|\,y)$ in the form

$$\int_0^x \mathrm{d}x\, u(x;t\,|\,y) + \int_x^{+\infty} \mathrm{d}x\, u(x;t\,|\,y) = 1 \tag{5.10}$$

we obtain

$$p_{\mathrm{R}}(x;t\,|\,y_1,y_2) + p_{\mathrm{L}}(x;t\,|\,y_1,y_2) = u(x;t\,|\,y_1) + u(x;t\,|\,y_2)\ . \tag{5.11}$$

Starting from Eq. (5.5), our reasoning has been valid for a general form of the external driving force $F(t) = \Gamma v(t)$ in (5.1). We remind that a negative instantaneous force pushes particles to the left, i.e., against the reflecting boundary at the origin. In this case, the force acts against the general spreading tendency stemming from the thermal Langevin force. A positive instantaneous force amplifies the diffusion in driving the particles to the right. Assuming the specific form of the driving force $F(t)$ (5.2), the most interesting physics emerges if the oscillating component $F_1 \sin(\omega t)$ superposes with a negative static force, i.e., if $F_1 > 0$, and $F_0 < 0$. *This case is treated in the rest of the thesis* (with one exception occurred in the beginning of the next Subsection).

5.1.1.1 Probability density at the boundary

Before embarking on the further discussion, let us collect some intuitively expected features of the probability density at the boundary. For the single-particle case, the solution of Eq. (5.6) has been discussed in [58]. Here we will review some of its properties and generalize the observations from [58] to the two-particle case with the hard-core interaction among the particles.

Taking $v_1 = 0$ or if $\omega = 0$ in the single-particle case, we have the standard diffusion problem with the time-independent drift and the reflecting boundary at the origin. In this case, the kernel in the integral equation (5.6) depends only on the time-difference $(t - t')$ and the Laplace-transformation method [63] readily yields the explicit solution [58]

$$u(0;t\,|\,y) = \frac{1}{\sqrt{\pi D t}} \exp\left[-\left(\frac{y + v_0 t}{\sqrt{4Dt}}\right)^2\right] - \frac{v_0}{D}\mathrm{erfc}\left(\frac{y + v_0 t}{\sqrt{4Dt}}\right)\ . \tag{5.12}$$

Here $\mathrm{erfc}(*)$ is the complementary error function [64]. The last formula is valid for any v_0. If $v_0 \geq 0$, the time-asymptotic value of the solution $\lim_{t\to+\infty} u(0;t\,|\,y)$ is zero because the particle gradually escapes far to the right from the boundary. On the other

hand, for any $v_0 < 0$ one has $\lim_{t\to+\infty} u(0;t\,|\,y) = |v_0|/D$. In this case, the force $|v_0|/\Gamma$ pushes the particle against the reflecting boundary. An arbitrary initial state relaxes to the equilibrium state $u^{(\mathrm{eq})}(x) = \theta(x)(|v_0|/D)\exp[-x|v_0|/D]$. What happens if the static force F_0 alone drives the two interacting particles?

The analogous reasoning remains valid for the two-particle case. However, the presence of the hard-core interaction alters the tagged particles probability densities at the boundary. Taking $x = 0$ in Eq. (5.8) and using the normalization of the function $u(x;t\,|\,y)$ lead to the probability density for the left particle at the boundary. We have

$$p_{\mathrm{L}}(0;t\,|\,y_1,y_2) = u(0;t\,|\,y_1) + u(0;t\,|\,y_2)\ . \tag{5.13}$$

This means that for any t, the value $p_{\mathrm{L}}(0;t\,|\,y_1,y_2)$ is either bigger then the corresponding quantity $u(x;t\,|\,y)$ in the single-particle case or zero if the both single-particle densities on the right hand side of Eq. (5.13) are zero. We can understand this as follows. Presently, in contrast to the diffusion without interaction, *two distinct forces* push the left particle against the reflecting boundary. One force is the external force $F(t)$. The second force, an *effective* one, originates from the hard-core interaction. Due to collisions, the right particle in an averaged sense pushes the left one against the barrier and thereby induces the increase of its probability density at the boundary[2]. If we set $v_0 \geq 0$ and $v_1 = 0$ or $\omega = 0$, the time-asymptotic value of the density (5.13) is zero because both particles escape far to the right from the boundary. For any $v_0 < 0$ and $v_1 = 0$ or $\omega = 0$, one has $\lim_{t\to+\infty} p_{\mathrm{L}}(0;t\,|\,y_1,y_2,0) = 2\,|v_0|/D$. The factor "2" here expresses an increase of the time-asymptotic value of the probability density due to the presence of the hard-core interaction.

On the contrary, the left particle in average pushes the right one away from the boundary. Thus one expects the value of the right particle's density at the boundary to be lowered in comparison to $u(0;t\,|\,y)$. In fact, due to the hard-core interaction, the right particle will never occur at the origin. After taking $x = 0$ in Eq. (5.11) and inserting there Eq. (5.13), we have

$$p_{\mathrm{R}}(0;t\,|\,y_1,y_2) = 0 \tag{5.14}$$

for all times $t \geq 0$. Note that this equality does not depend on the drift $v(t)$.

Returning to the oscillating force (5.2) with $F_1 > 0$ and $\omega > 0$, assume again the static force component directed towards the reflecting barrier $F_0 < 0$. Then the solution of the integral equation (5.6) represents a fairly nontrivial problem. There are two sources of difficulties. Firstly, the kernel $g(0;t\,|\,0;t')$ in Eq. (5.6) displays a weak singularity at the upper integration limit. Secondly and more importantly, this kernel

[2]On the other words, the hard core interaction induces an *anomalous drift*. For an unconstrained diffusion this drift is in detail discussed in [65].

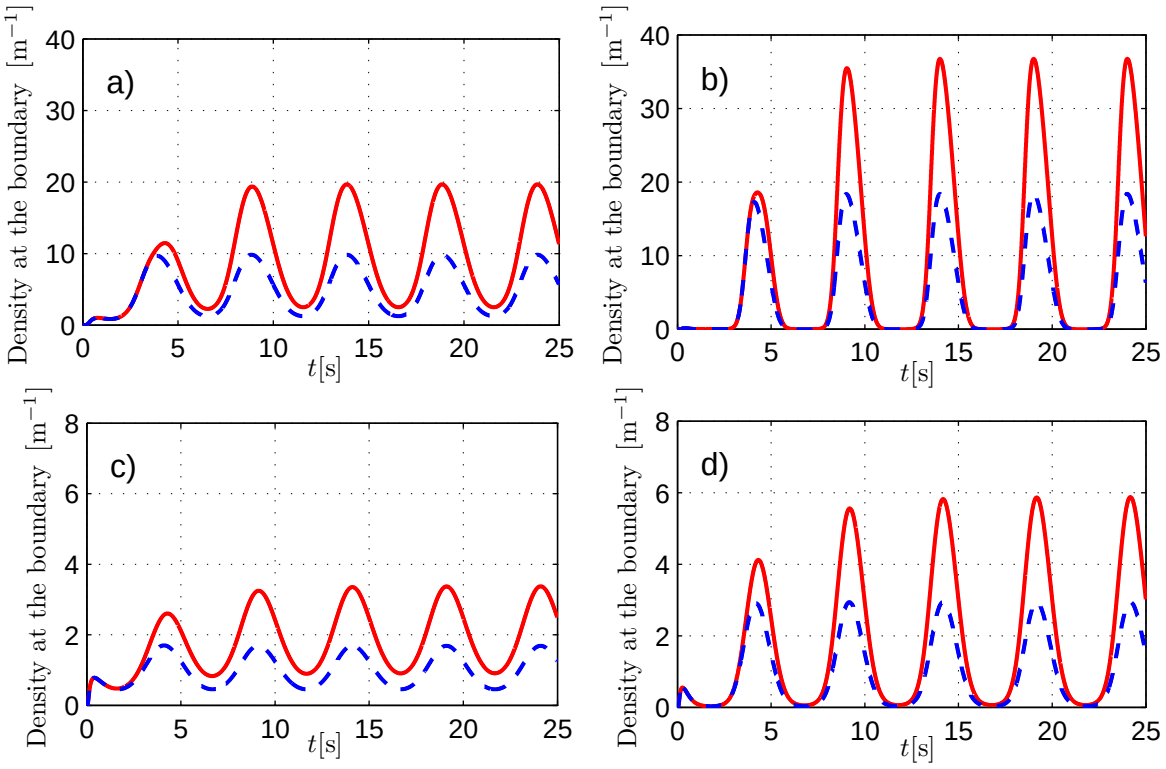

Figure 5.1: Probability densities at the position of the reflecting boundary as the function of time. In all panels the dashed (blue) curve represents the density $u(0;t\,|\,y_1)$, as obtained by the numerical solution of the integral equation (5.6). The full (red) curve corresponds to the case with hard-core interaction, i.e., the density $p_{\mathrm{L}}(0;t\,|\,y_1,y_2)$. Notice the interaction-induced increment of the value $p_{\mathrm{L}}(0;t\,|\,y_1,y_2)$ as discussed in the main text. The parameters used in the panels are a) $v_0=-1.0\,\mathrm{m\,s^{-1}}$, $v_1=1.0\,\mathrm{m\,s^{-1}}$, $D=0.2\,\mathrm{m^2 s^{-1}}$, $\omega=0.4\,\pi\mathrm{rad\,s^{-1}}$, b) $v_0=-1.0\,\mathrm{m\,s^{-1}}$, $v_1=3.0\,\mathrm{m\,s^{-1}}$, $D=0.2\,\mathrm{m^2 s^{-1}}$, $\omega=0.4\,\pi\mathrm{rad\,s^{-1}}$, c) $v_0=-1.0\,\mathrm{m\,s^{-1}}$, $v_1=1.0\,\mathrm{m\,s^{-1}}$, $D=1.0\,\mathrm{m^2 s^{-1}}$, $\omega=0.4\,\pi\mathrm{rad\,s^{-1}}$, d) $v_0=-1.0\,\mathrm{m\,s^{-1}}$, $v_1=3.0\,\mathrm{m\,s^{-1}}$, $D=1.0\,\mathrm{m^2 s^{-1}}$, $\omega=0.4\,\pi\mathrm{rad\,s^{-1}}$. Initial positions in all panels are $y_1=1.0\,\mathrm{m}$, $y_2=5.0\,\mathrm{m}$.

is not of the convolution type. This observation rules out the application of the Laplace transformation method. Equations of this type have been already investigated in the mathematical literature. As for their numerical solution, we have implemented the so called Product Integration method [67] which includes a special treatment of the weak singularity in Eq. (5.6).

Let us now place two particles at the time zero, the first particle at the position

$y_1 = 1$ m, the second one at $y_2 = 5$ m. The evolution of the *left* particle's probability density at the boundary is illustrated in Fig. 5.1 for four different values of the parameters. Each one of the four panels depicts two functions of time. The dashed (blue) curve describes the density in the case without interaction among the particles, i.e., the function $u(0;t\,|\,y_1)$, as obtained by the numerical solution of the integral equation (5.6). The full (red) curve corresponds to the case with the hard-core interaction among the particles. It represents the density $p_{\mathrm{L}}(0;t\,|\,y_1,y_2)$ obtained from the solution of Eq. (5.6) via Eq. (5.13).

Comparison of panels a) and c) (or b) and d)) illustrates the influence of increasing temperature. The amplitude of the oscillations decreases since the density is more delocalized. This is true for both the case with and the case without the interaction. Notice that there exist an instant (in all panels within the interval $t \in [0,5]$ s), until which both oscillating densities are taking the same values as the functions of time. Position of this point on the time axis depends on the distance between the particles at $t = 0$ and the bath temperature. It indicates an instant when the left particle starts to realize the presence of the right particle (in a statistical sense). The higher is the temperature the more motile are both particles. Their probability densities spread faster, hence the effect of the interaction occurs earlier. During the time interval depicted on the time axis, the external force has made five full cycles. During the first half-period of any of the cycle the force has pushed the particle to the right from the boundary. This implies a delayed decrease of the probability density at the boundary. If there is a phase shift in the input force, the response would also acquire a corresponding phase shift but its amplitude would remain unchanged.

Comparison of panels a) and b) (or c) and d)) demonstrates the influence of increasing of the amplitude F_1 of the external force. The oscillations are more pronounced and the response exhibits strong nonlinear features. Generally speaking, a highly non-equilibrium stationary regime occurs whenever the ratio F_1/F_0 is greater than one, the temperature is low, and the frequency of the force modulation is small.

Fig. 5.1 illustrates another important feature of the driven diffusion process. Transient effects in the dynamics of the density are very short-lived in their nature. They subside very rapidly (after few periods) and the system settles down to the *stationary (time-asymptotic) regime*. As usually, the stationary regime per se includes the most important physics in the problem. Is it possible to deduce the time-asymptotic dynamics directly from the integral equation (5.6)? This question has been thoroughly investigate in [59] and we now quote the results thereof which are relevant in the present context.

In [59] it was shown that the (time-asymptotic) probability density at the boundary in the stationary regime (for a single-diffusing particle) can be represented by the Fourier

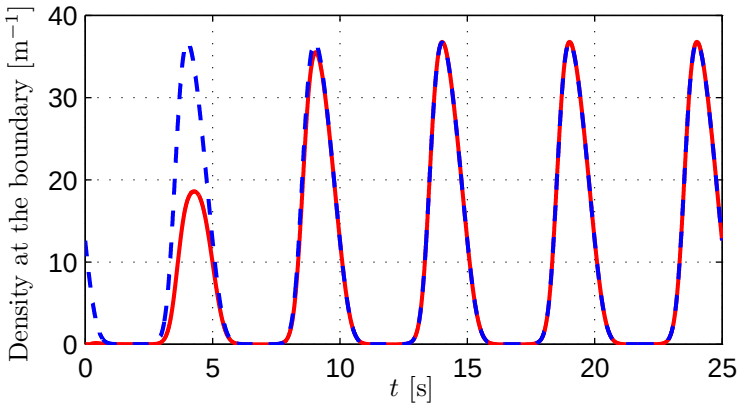

Figure 5.2: Comparison of the density $p_{\mathrm{L}}(0,t\,|\,y_1,y_2)$, as obtained by the numerical solution of the integral equation (5.6) via Eq. (5.13) (the full red curve) with the exact asymptotic density $\tilde{p}_{\mathrm{L}}(0;t)$ computed from Eq. (5.18) (the dashed blue curve). Parameters used (same as in the panel b) in Fig. 5.1) are $v_0 = -1.0\,\mathrm{m\,s^{-1}}$, $v_1 = 3.0\,\mathrm{m\,s^{-1}}$, $D = 0.2\,\mathrm{m^2 s^{-1}}$, $\omega = 0.4\,\pi\,\mathrm{rad\,s^{-1}}$, $y_1 = 1.0\,\mathrm{m}$, $y_2 = 5.0\,\mathrm{m}$.

series

$$\tilde{u}(0;t) = \frac{|v_0|}{D}\left\{1 + 2\sum_{k=1}^{\infty}|f_k|\cos\left[k\omega t - \arctan\left(\frac{\mathrm{Im}f_k}{\mathrm{Re}f_k}\right)\right]\right\}\ . \tag{5.15}$$

Here and below in this Section the tilde above a symbol points out that the corresponding quantity describes the dynamics in the above-mentioned asymptotic regime. In Eq. (5.15) we have introduced the *complex amplitudes* f_k which in standard matrix notation are given as

$$f_k = \left\langle k\,|\,\mathbb{R}_{-+}^{-1}\,|\,0\right\rangle\ , \quad k = 0, \pm1, \pm2, \ldots\ , \tag{5.16}$$

where $\mathbb{R}_{-+}^{-1}$ denotes an inverse matrix to the matrix $\mathbb{R}_{-+}$ with entries

$$\langle m\,|\,\mathbb{R}_{-+}\,|\,n\rangle = \mathrm{I}_{|m-n|}(-\kappa\sqrt{1-\mathrm{i}m\zeta}+\kappa) \quad m, n = 0, \pm1, \pm2, \ldots\ , \tag{5.17}$$

where $\mathrm{I}_m(x)$ is the modified Bessel function of the first kind [64]. Moreover, we have introduced the *scaled frequency* $\zeta = 4\omega D/v_0^2$ and the *scaled amplitude* of the oscillating force $\kappa = |v_0|v_1/(2\omega D)$.

In the case with interaction, the time-asymptotic probability density of the right particle's position at the boundary is always zero (cf. Eq. (5.14)). The asymptotic density of the left particle's position at the boundary according to Eq. (5.13) reads

$$\tilde{p}_{\mathrm{L}}(0;t) = 2\tilde{u}(0;t) = 2\frac{|v_0|}{D}\left\{1 + 2\sum_{k=1}^{\infty}|f_k|\cos\left[k\omega t - \arctan\left(\frac{\mathrm{Im}f_k}{\mathrm{Re}f_k}\right)\right]\right\}\ . \tag{5.18}$$

Turning to the numerical analysis of analytical result (5.18), the complex amplitudes f_k have been calculated via direct numerical inversion of the matrix $\mathbb{R}_{-+}$. Of course, the infinite-order matrix must be first reduced onto its finite-order central block. The entries of the reduced matrix are again given by Eq. (5.17), presently, however, $m, n = 0, \pm 1, \pm 2, ..., \pm M$. The integer M has been taken large enough such that its further increase does not change the result within a predefined precision. In this sense all numerical results obtained from exact analytical solutions represent the exact long-time solution of the problem in question. Fig. 5.2 shows the comparison of exact result (5.18) with the function (5.13) which was obtained by the numerical solution of the integral equation (5.6). The comparison of this functions could also serve as the estimation of the duration of transient effects.

5.1.1.2 Space-resolved probability densities

Up to now, we have only discussed the time-dependence of probability densities at the boundary. In this Paragraph, we focus on the time- and space-resolved probability densities of particle's coordinates.

We remind that, regardless of the initial condition, a time-independent drift towards the origin induces the gradual constitution of the unique equilibrium density which in the single-particle case reads $u^{(\mathrm{eq})}(x) = \theta(x)(|v_0|/D)\exp[-x|v_0|/D]$. Thereupon (cf. Eq. (5.4)), for the two interacting particles simultaneous the equilibrium density is $p^{(2)}_{\mathrm{eq}}(x_1, x_2) = \theta(x_2 - x_1)(|v_0|/D)^2 \exp[-(x_1 + x_2)|v_0|/D]$.

Consider again the oscillating force $F(t)$ with amplitudes $F_0 < 0$ and $F_1 > 0$, place the particles on the initial positions y_1 and y_2 and start up the time-evolution. During a certain incipient time-interval, the dynamics of the system will be strongly affected by the initial positions y_1 and y_2. This affect is getting weaker and weaker as the time goes. Finally, the system settles down to the unique time-asymptotic dynamics, regardless the initial positions. The analysis of the *transient effects*, i.e., of the system's relaxation into the time-asymptotic dynamics, can be numerically carried out as follows. We simply insert the density $u(0; t \,|\, y)$ obtained by the Product Integration method into Eq. (5.7) and carry out the corresponding integration over the time. Thereby we get the probability density $u(x; t \,|\, y)$ as the function of x and t. In order to obtain the marginal probability density $p_{\mathrm{L}}(x; t \,|\, y_1, y_2)$ ($p_{\mathrm{R}}(x; t \,|\, y_1, y_2)$) of the position of the left (right) particle, we insert the densities $u(x; t \,|\, y_1)$, $u(x; t \,|\, y_1)$ into Eq. (5.4) and carry out the (numerical) integration of the function $p^{(2)}(x_1, x_2; t \,|\, y_1, y_2)$ over the coordinate x_2 (x_1) as has been pointed out in Eq. (5.8) (Eq. (5.9)).

Densities obtained exactly in that way are shown in Fig.5.3 within two periods of the driving force. Notice that each panel in Fig. 5.3 has a different scale. The density

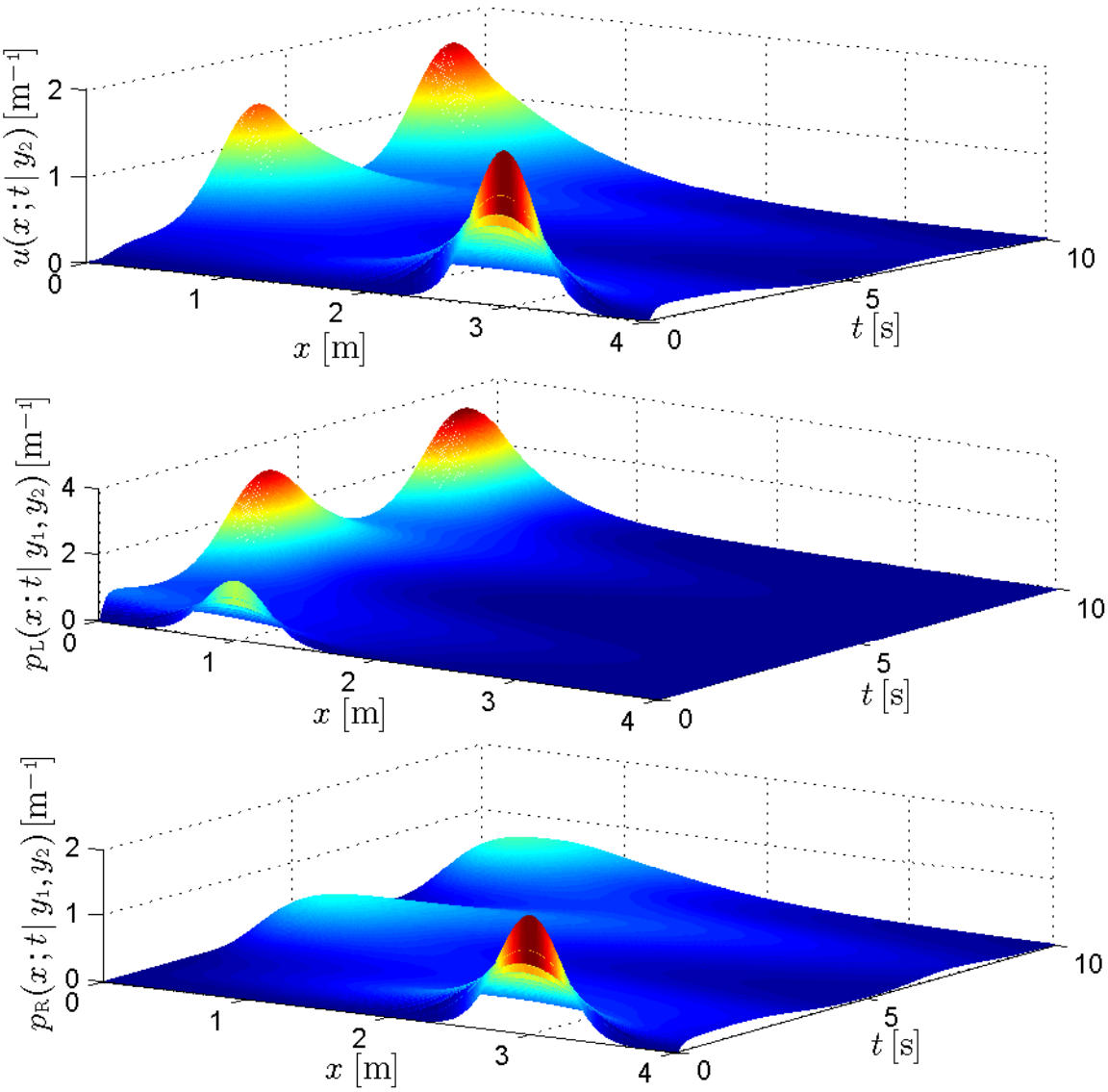

Figure 5.3: Time- and space-resolved probability densities for the first two periods of the driving force ($x \in [0,4]$ m, $t \in [0.025, 10]$ s). The parameters used are $v_0 = -1.0\,\mathrm{m\,s^{-1}}$, $v_1 = 1.0\,\mathrm{m\,s^{-1}}$, $D = 1.0\,\mathrm{m^2 s^{-1}}$, $\omega = 0.4\,\pi\mathrm{rad\,s^{-1}}$, initial positions of the particles are $y_1 = 1\,\mathrm{m}$, $y_2 = 3\,\mathrm{m}$.

$p_{\mathrm{R}}(x;t\,|\,y_1,y_2)$ is always zero at the boundary as it should be according to Eq. (5.14). Left particle's density $p_{\mathrm{L}}(x;t\,|\,y_1,y_2)$ is localized closer to the origin and takes higher values than the single-particle density $u(x;t\,|\,y_2)$.

However, this numerical approach is highly time-consuming, hence it is unsuitable for the analysis of the time-asymptotic regime. Fortunately, the knowledge of the complex amplitudes f_k (5.16) allows for a rather detailed discussion of many features of the emerging diffusion process. Presently, we consider the time-asymptotic dynamics of the system and derive exact analytical results for the probability densities.

In the time-asymptotic regime, the single-particle probability density $\tilde{u}(x;t)$ does not depend on the initial condition (as was earlier represented by the variable y). At any fixed point $x \geq 0$ it exhibits oscillations with the fundamental frequency ω. According to Eq. (5.4) the two-particle probability density in the case with interaction in the asymptotic regime reads

$$\tilde{p}^{(2)}(x_1,x_2;t) = 2\theta(x_2-x_1)\tilde{u}(x_1\,;t)\tilde{u}(x_2\,;t)\ . \tag{5.19}$$

This density also exhibits oscillations with the frequency ω at any points $x_1 \geq 0, x_2 \geq 0$ for which the inequality $x_1 < x_2$ holds, otherwise it equals to zero. In agreement with Eq. (5.8) and Eq. (5.9), the probability densities of the positions of the left and right particle in the time-asymptotic regime read

$$\tilde{p}_{\mathrm{L}}(x;t) \;=\; \int_0^{+\infty} \mathrm{d}x_2\, \tilde{p}^{(2)}(x,x_2;t)\ , \tag{5.20}$$

$$\tilde{p}_{\mathrm{R}}(x;t) \;=\; \int_0^{+\infty} \mathrm{d}x_1\, \tilde{p}^{(2)}(x_1,x;t)\ , \tag{5.21}$$

respectively.

We expand the single-particle asymptotic density into the Fourier series

$$\tilde{u}(x;t) = \sum_{k=-\infty}^{+\infty} u_k(x)\exp(-\mathrm{i}k\omega t)\ . \tag{5.22}$$

Notice that the Fourier coefficients $u_k(x)$ depend on the coordinate x. As it is shown in [59] we can express this coefficients as

$$u_k(x) = \frac{|v_0|}{D}\,\langle k\,|\,\mathbb{L}_{--}\mathbb{E}(x)\mathbb{R}_{++}\,|\,f\rangle\ \ , \quad k=0,\pm1,\pm2,\ldots\ . \tag{5.23}$$

Here $|f\rangle$ i is the column vector of the complex amplitudes, i.e., $f_k = \langle k\,|\,f\rangle$, $\mathbb{E}(x)$ denotes diagonal matrix with complex, x-dependent elements

$$\langle m\,|\,\mathbb{E}(x)\,|\,n\rangle = \frac{\delta_{n\,m}}{2}\left[1+\frac{1}{\sqrt{1-\mathrm{i}m\zeta}}\right]\exp\left[-x\frac{|v_0|}{2D}\left(\sqrt{1-\mathrm{i}m\zeta}+1\right)\right]\ , \tag{5.24}$$

and $\mathbb{L}_{--}, \mathbb{R}_{++}$ are two matrices with entries

$$\langle m \,|\, \mathbb{L}_{--} \,|\, n \rangle = \mathrm{I}_{|m-n|}(-\kappa\sqrt{1-\mathrm{i}n\zeta} - \kappa) \ , \tag{5.25}$$

$$\langle m \,|\, \mathbb{R}_{++} \,|\, n \rangle = \mathrm{I}_{|m-n|}(+\kappa\sqrt{1-\mathrm{i}m\zeta} + \kappa) \ , \tag{5.26}$$

where m and n are integers.

Let us now expand into the Fourier series the asymptotic simultaneous two-particle probability density $\tilde{p}^{(2)}(x_1, x_2; t)$. We have

$$\tilde{p}^{(2)}(x_1, x_2; t) = 2\theta(x_2 - x_1) \sum_{k=-\infty}^{+\infty} u_k^{(2)}(x_1, x_2) \exp(-\mathrm{i}k\omega t) \ . \tag{5.27}$$

Presently, notice that the Fourier coefficients $u_k^{(2)}(x_1, x_2)$ depend on the coordinates of both particles. On the other hand, after expanding both single-particle densities in Eq. (5.19) according to Eq. (5.22), we have

$$\tilde{p}^{(2)}(x_1, x_2; t) = 2\theta(x_2 - x_1) \sum_{m=-\infty}^{+\infty} \sum_{n=-\infty}^{+\infty} u_m(x_1) u_n(x_2) \exp(-\mathrm{i}m\omega t) \exp(-\mathrm{i}n\omega t) \ . \tag{5.28}$$

Hence it is possible to express the unknown Fourier coefficients $u_k^{(2)}(x_1, x_2)$ in Eq. (5.27) in terms of the known coefficients $u_k(x)$ (5.23). After invoking the substitution $m+n = k$ in the summation index m in Eq. (5.28) we obtain

$$\tilde{p}^{(2)}(x_1, x_2; t) = 2\theta(x_2 - x_1) \sum_{k=-\infty}^{+\infty} \left[\sum_{n=-\infty}^{+\infty} u_{k-n}(x_1) u_n(x_2) \right] \exp(-\mathrm{i}k\omega t) \ . \tag{5.29}$$

If we compare Eq. (5.29) with Eq. (5.27), we get

$$u_k^{(2)}(x_1, x_2) = \sum_{n=-\infty}^{+\infty} u_{k-n}(x_1) u_n(x_2) \, , \quad k = 0, \pm 1, \pm 2, \ldots \ . \tag{5.30}$$

Thus the Fourier coefficients $u_k^{(2)}(x_1, x_2)$ are given as the discrete convolutions of the Fourier coefficients $u_k(x)$ (5.23).

Notice that the convolution (5.30) is symmetric under the change of the particle's coordinates, i.e., $u_k^{(2)}(x_1, x_2) = u_k^{(2)}(x_2, x_1)$. Moreover, the only x-dependent terms in the matrix product (5.23) arise from the entries of the matrix $\mathbb{E}(x)$ (5.24). This two

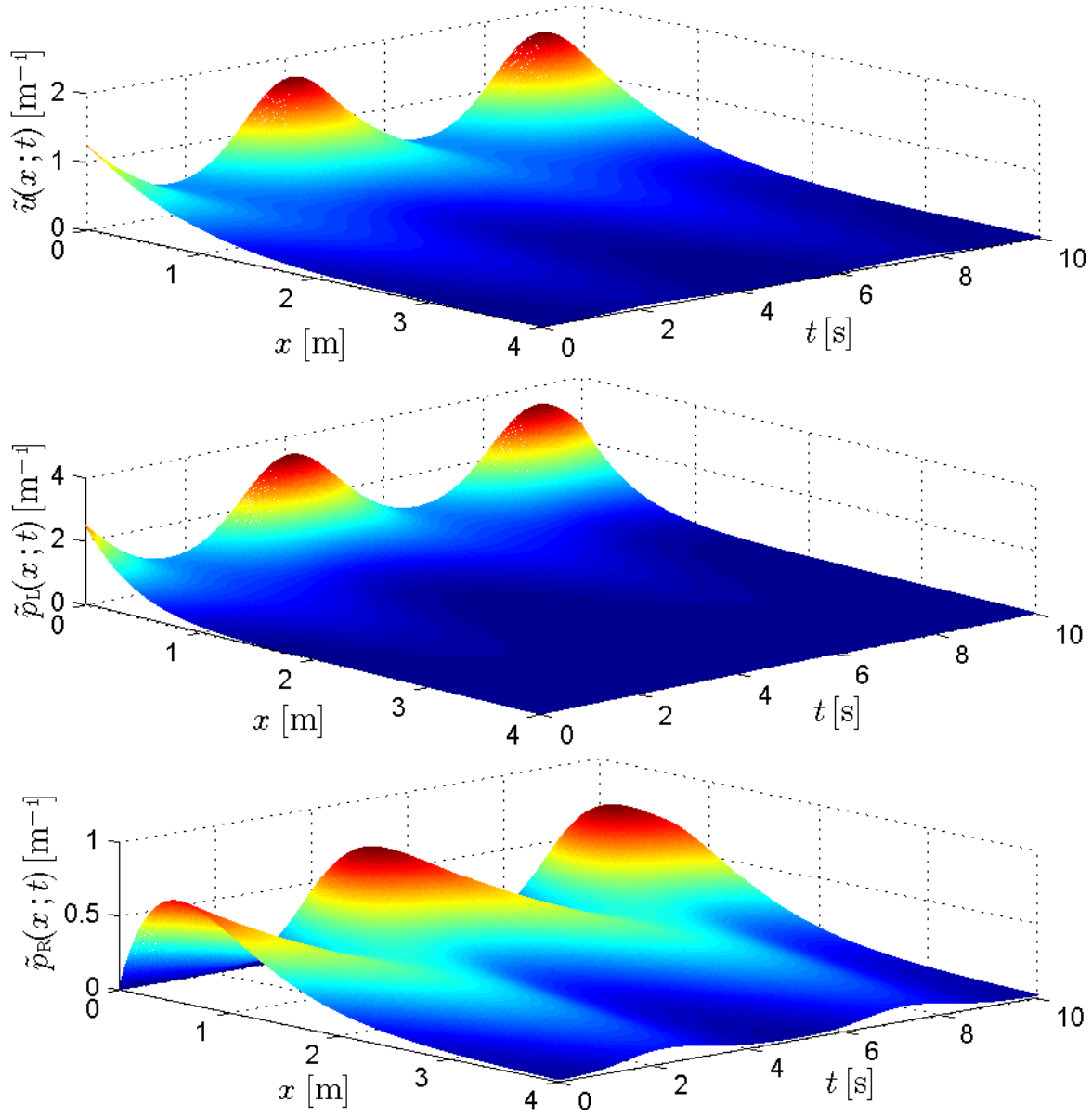

Figure 5.4: Time- and space-resolved probability densities in the time-asymptotic regime. We have used the same set of parameters as in Fig. 5.3, i.e., $v_0 = -1.0\,\mathrm{m\,s^{-1}}$, $v_1 = 1.0\,\mathrm{m\,s^{-1}}$, $D = 1.0\,\mathrm{m^2 s^{-1}}$, $\omega = 0.4\,\pi\mathrm{rad\,s^{-1}}$.

observations yield to the explicit expressions of the tagged-particle's probabilities (5.20), (5.21). If we define the coefficients

$$l_k(x) = \frac{|v_0|}{D} \langle k \,|\, \mathbb{L}_{--}\mathbb{E}_{\rm L}(x)\mathbb{R}_{++} \,|\, f\rangle \ , \quad k = 0, \pm 1, \pm 2, ... \ , \tag{5.31}$$

$$r_k(x) = \frac{|v_0|}{D} \langle k \,|\, \mathbb{L}_{--}\mathbb{E}_{\rm R}(x)\mathbb{R}_{++} \,|\, f\rangle \ , \quad k = 0, \pm 1, \pm 2, ... \ , \tag{5.32}$$

where two diagonal matrices $\mathbb{E}_{\rm L}(x) \equiv \int_x^{+\infty} {\rm d}x' \mathbb{E}(x')$, $\mathbb{E}_{\rm R}(x) \equiv \int_0^x {\rm d}x' \mathbb{E}(x')$ possess the matrix elements

$$\langle m \,|\, \mathbb{E}_{\rm L}(x) \,|\, n\rangle = \frac{D}{|v_0|} \frac{\delta_{n\,m}}{\sqrt{1 - {\rm i}m\zeta}} \exp\left[-x \frac{|v_0|}{2D} \left(\sqrt{1 - {\rm i}m\zeta} + 1 \right) \right] \ , \tag{5.33}$$

$$\langle m \,|\, \mathbb{E}_{\rm R}(x) \,|\, n\rangle = \frac{D}{|v_0|} \frac{\delta_{n\,m}}{\sqrt{1 - {\rm i}m\zeta}} \left\{ 1 - \exp\left[-x \frac{|v_0|}{2D} \left(\sqrt{1 - {\rm i}m\zeta} + 1 \right) \right] \right\} \ , \tag{5.34}$$

where m and n are integers. Then the marginal densities (5.20), (5.21) read

$$\tilde{p}_{\rm L}(x;t) = 2 \sum_{k=-\infty}^{+\infty} \left[\sum_{n=-\infty}^{+\infty} u_{k-n}(x)\, l_n(x) \right] \exp(-{\rm i}k\omega t) \ , \tag{5.35}$$

$$\tilde{p}_{\rm R}(x;t) = 2 \sum_{k=-\infty}^{+\infty} \left[\sum_{n=-\infty}^{+\infty} u_{k-n}(x)\, r_n(x) \right] \exp(-{\rm i}k\omega t) \ . \tag{5.36}$$

Let us now focus on the numerical analysis of the asymptotic probability densities $\tilde{p}_{\rm L}(x;t)$ (5.35), $\tilde{p}_{\rm R}(x;t)$ (5.36) and $\tilde{u}(x;t)$ (5.22). Presently, we have to reduce both the vector of the complex amplitudes $|f\rangle$ and the matrices $\mathbb{L}_{--}$, $\mathbb{R}_{++}$, $\mathbb{E}(x)$, $\mathbb{E}_{\rm L}(x)$ and $\mathbb{E}_{\rm R}(x)$. Except for this controllable approximation, we can already reconstruct the full time- and space-resolved non-linear "waves" of the probability densities, as represented by the functions $\tilde{u}(x;t)$, $\tilde{p}_{\rm L}(x;t)$, $\tilde{p}_{\rm R}(x;t)$. Fig. 5.4 illustrates these time-asymptotic densities within two periods of the external driving force.

5.1.2 Mean position

Let us now focus on the mean positions of particles. If $F_0 < 0$ and $F_1 = 0$, the probability density of the single diffusing particle relaxes to the exponential form

$$u^{(\rm eq)}(x) = \theta(x) \frac{|v_0|}{D} \exp\left(-x \frac{|v_0|}{D} \right) \ . \tag{5.37}$$

In this case, the equilibrium density of the left particle reads

$$p_{\mathrm{L}}^{(\mathrm{eq})}(x) = 2\theta(x)\frac{|v_0|}{D}\exp\left(-2x\frac{|v_0|}{D}\right) \ . \tag{5.38}$$

The only difference between this two densities is factor "2" which occurs in the exponential and as the multiplicative prefactor in $p_{\mathrm{L}}^{(\mathrm{eq})}(x)$. It evokes that $p_{\mathrm{L}}^{(\mathrm{eq})}(x)$ takes higher value at the boundary and decreases more rapidly as the coordinate x growth as compared with $u^{(\mathrm{eq})}(x)$. Thus an impact of the interaction on the left tagged particle in the equilibrium state is equivalent to the replacement of the ratio $|v_0|/D$ by $2|v_0|/D$ in the equilibrium density. For instance we could simply double the slope of the potential or lower the temperature two times.

However, the impact of the interaction on the right tagged particle's equilibrium density could not be expressed so simply. This density reads

$$p_{\mathrm{R}}^{(\mathrm{eq})}(x) = 2\theta(x)\frac{|v_0|}{D}\exp\left(-x\frac{|v_0|}{D}\right)\left[1-\exp\left(-x\frac{|v_0|}{D}\right)\right] \ . \tag{5.39}$$

It is zero at the boundary and possesses the maximum value $p_{\mathrm{R}}^{(\mathrm{eq})}(x_{\mathrm{m}}) = |v_0|/(2D)$ at the point $x_{\mathrm{m}} = D\log(2)/|v_0|$. Thus, the maximum value of the density $p_{\mathrm{R}}^{(\mathrm{eq})}(x)$ is higher and it is located closer to the boundary as the ratio $|v_0|/D$ is increased. For big values of $|v_0|/D$, the equilibrium densities $u^{(\mathrm{eq})}(x)$, $p_{\mathrm{L}}^{(\mathrm{eq})}(x)$ and $p_{\mathrm{R}}^{(\mathrm{eq})}(x)$ are localized close to the reflecting boundary. On the contrary, the smaller is the ratio $|v_0|/D$, the more delocalized are equilibrium densities $u^{(\mathrm{eq})}(x)$, $p_{\mathrm{L}}^{(\mathrm{eq})}(x)$, $p_{\mathrm{R}}^{(\mathrm{eq})}(x)$.

The mean positions of the particles in the equilibrium approach values $\mu^{(\mathrm{eq})} = D/|v_0|$, $\mu_{\mathrm{L}}^{(\mathrm{eq})} = D/(2|v_0|)$, $\mu_{\mathrm{R}}^{(\mathrm{eq})} = 3D/(2|v_0|)$ in the case of the single diffusing particle, left particle and right particle respectively. Notice that all mean position are linear functions of the ration $D/|v_0|$ and the relation $\mu_{\mathrm{L}}^{(\mathrm{eq})} + \mu_{\mathrm{R}}^{(\mathrm{eq})} = 2\mu^{(\mathrm{eq})}$ holds.

Turning to the case with the modulated force, the mean positions are defined as the first moments of the corresponding probability densities. Hence, the mean position of the single diffusing particle reads

$$\tilde{\mu}(t) = \int_0^{+\infty} \mathrm{d}x\, x\, \tilde{u}(x;t) \ . \tag{5.40}$$

In the case with interaction, the mean position of the left particle and the mean position of the right one read

$$\tilde{\mu}_{\mathrm{L}}(t) = \int_0^{+\infty} \mathrm{d}x\, x\, \tilde{p}_{\mathrm{L}}(x;t) \ , \tag{5.41}$$

$$\tilde{\mu}_{\mathrm{R}}(t) = \int_0^{+\infty} \mathrm{d}x\, x\, \tilde{p}_{\mathrm{R}}(x;t) \ , \tag{5.42}$$

respectively. Let us now derive the exact analytical expressions for the mean positions (5.40), (5.41), and (5.42).

Owing to the oscillatory driving force, the mean positions of the particles will oscillate with the fundamental frequency ω. The mean position of the single diffusing particle can be represented by the Fourier series

$$\tilde{\mu}(t) = \sum_{k=-\infty}^{+\infty} \mu_k \exp(-\mathrm{i}k\omega t) \ . \tag{5.43}$$

After inserting Eq. (5.43) into Eq. (5.40) and carrying out the integration we obtain the Fourier coefficients μ_k. They read

$$\mu_k = \frac{D}{|v_0|} \langle k \,|\, \mathbb{L}_{--} \mathbb{K} \, \mathbb{R}_{++} \,|\, f \rangle \ , \quad k = 0, \pm 1, \pm 2, ... \ , \tag{5.44}$$

where the matrix $\mathbb{K} \equiv (v_0/D)^2 \int_0^{+\infty} \mathrm{d}x \, x \, \mathbb{E}(x)$ possess the matrix elements

$$\langle m \,|\, \mathbb{K} \,|\, n \rangle = \frac{2 \, \delta_{n\,m}}{1 - \mathrm{i}m\zeta + \sqrt{1 - \mathrm{i}m\zeta}} \ , \tag{5.45}$$

where m and n are integers. Matrices $\mathbb{L}_{--}$, $\mathbb{R}_{++}$ are defined in Eq. (5.25), Eq. (5.26) respectively and $f_k = \langle k \,|\, f \rangle$ are the complex amplitudes (5.16).

The Fourier series representations of the mean positions (5.41) and (5.42) read

$$\tilde{\mu}_{\mathrm{L}}(t) = \sum_{k=-\infty}^{+\infty} \lambda_k \exp(-\mathrm{i}k\omega t) \ , \tag{5.46}$$

$$\tilde{\mu}_{\mathrm{R}}(t) = \sum_{k=-\infty}^{+\infty} \rho_k \exp(-\mathrm{i}k\omega t) \ , \tag{5.47}$$

with the Fourier coefficients given as the space integration of x times the convolution which occurs in the tagged particle densities (5.36), (5.35). We have

$$\lambda_k = 2 \sum_{n=-\infty}^{+\infty} \int_0^{+\infty} \mathrm{d}x \, x \, u_{k-n}(x) l_n(x) \ , \tag{5.48}$$

$$\rho_k = 2 \sum_{n=-\infty}^{+\infty} \int_0^{+\infty} \mathrm{d}x \, x \, u_{k-n}(x) r_n(x) \ , \tag{5.49}$$

The mean positions are intimately related to the mean energies of the particles, work done on the particles by an external agent and heat released to the heat bath. We elucidate these relations in the next Section. Moreover, we will show that work and heat per one period can be expressed as the real parts of the first Fourier coefficients μ_1, λ_1, and ρ_1 (except for a trivial multiplicative prefactor). The zero Fourier coefficients μ_0, λ_0, and ρ_0 also possess a certain physical interpretation. The meaning and properties of the zero Fourier coefficient μ_0, i.e., the zero coefficient for the single diffusing particle, were deeply discussed in [58, 59]. This coefficient is always real and represents the *stationary mean position* of the particle, i.e. the mean position averaged over the period of the driving force. We have

$$\mu_0 = \frac{\omega}{2\pi} \int_0^{2\pi/\omega} \mathrm{d}t \, \tilde{\mu}(t) \ . \tag{5.50}$$

Moreover in [59] was shown that

$$\mu_0 = \frac{D}{|v_0|} \left(1 + 2\kappa \mathrm{Re} f_1\right) \ . \tag{5.51}$$

This stationary mean position is always greater than the equilibrium mean position $\mu^{(\mathrm{eq})} = D/|v_0|$. The difference $\mu_0 - \mu^{(\mathrm{eq})} = v_1 \mathrm{Re} f_1/\omega$ increases with the amplitude F_1 of the modulated force and always decreases with increasing of both the frequency ω and the bath temperature T [58]. The mean position may be interpreted as the "centre of mass" of the probability density. Thus the oscillatory driving force in average shifts the probability density (or the concentration of the particles) away from the boundary[3]. In the case with interaction, stationary mean position of the particles are λ_0 and ρ_0. Unfortunately, the derivation of the relations similar to (5.51) for this functions appears as the fairly non-trivial problem. However, from the numerical analysis we know that all qualitative features named above for the single-particle diffusion remain valid also for the diffusion of interacting particles.

We proceed with numerical analysis of the time-dependent mean positions (5.43), (5.46), and (5.47). Fig. 5.5 confronts these functions as computed for two different values of the parameters within two periods of the driving force. The parameters differ only in the amplitudes F_1 of the modulated force. In panels a! 1) and a! 2), the magnitudes of the modulated and time-independent parts of the force are equal, i.e., $F_1 = |F_0|$. Hence the driving force is always non-positive. Up to the instant $t_1 = \pi/(2\omega)$ (within one period) it always pushes the particles to the left, against the reflecting boundary. At the instant t_1 the force is zero. Induced oscillations of the mean positions (see panel

[3] An approach to the investigation of the *dynamical shift* $\mu_0 - \mu^{(\mathrm{eq})}$ in [58, 59] was based rather on the asymptotic analysis of Eq. (5.7) than on the properties of the expression (5.44).

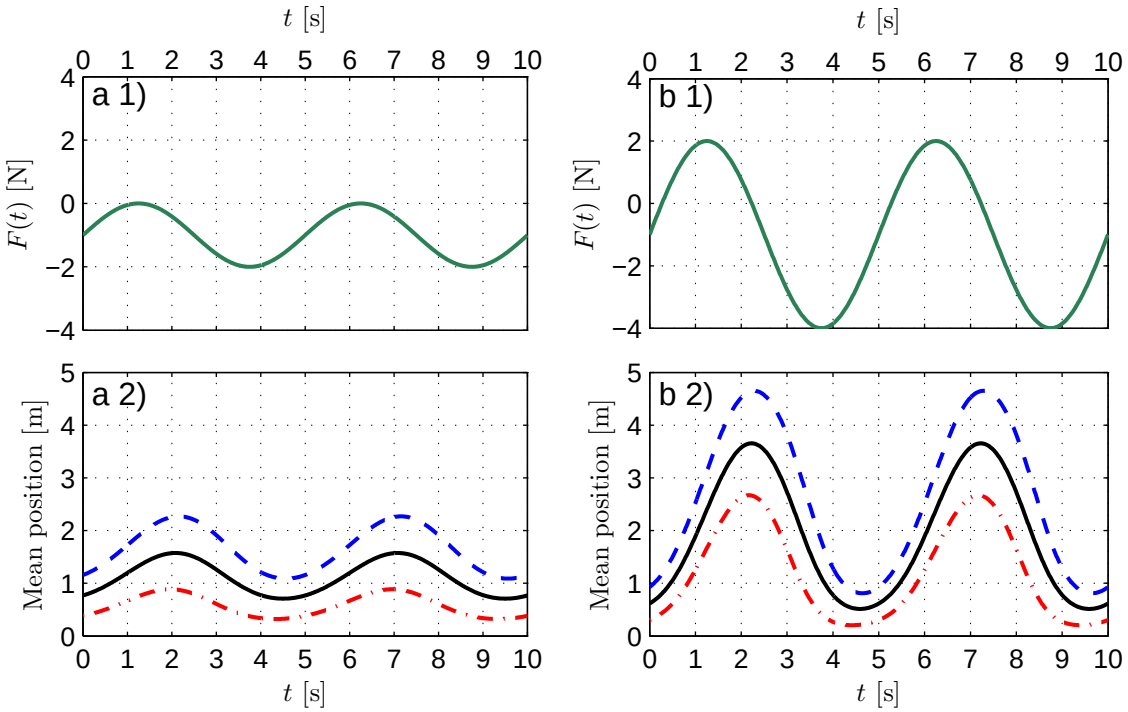

Figure 5.5: Mean positions as the functions of time. The curves in the upper panels show the time-dependency of the driving force (5.2). The oscillations of the mean positions are shown in the lower panels always bellow the corresponding driving force. The solid black line show the mean positions $\tilde{\mu}(t)$, the dashed blue line show the mean positions $\tilde{\mu}_{\mathrm{R}}(t)$ and the dot-dashed red line show $\tilde{\mu}_{\mathrm{L}}(t)$. In the panels a 1) and a 2) we take $F_1 = 1.0\,\mathrm{N}$, in the panels b 1) and b 2) we take $F_1 = 3.0\,\mathrm{N}$. The static component $F_0 = -1.0\,\mathrm{N}$, the frequency $\omega = 0.4\,\pi\,\mathrm{s}^{-1}$, and the diffusion constant $D = 1.0\,\mathrm{m}^2\mathrm{s}^{-1}$ are the same in all panels.

a 2)) exhibit phase differences with each other and with the driving force in the sense that they take their maximum values at the different times within the period.

As the amplitude F_1 of the modulated force is increased, the force $F(t)$ becomes positive for a certain time-interval within the period. This situation is illustrated in the panel b 1) of Fig. 5.5. The positive force pushes particles to the right, so the particles will attain to the larger distances from the boundary than in the case $F_1 = |F_0|$. Consequently, maxima of the mean positions within the period will attain to larger values (compare panels a 2) and b 2)). Notice that two interacting particles in an averaged sense will be both farther from the origin and farther from each other. On the other hand as the amplitude F_1 of the modulated force is increased, the maximum magnitude

of the force $F(t)$ in the direction towards the boundary is increased as well. Thus the particles will attain not only farther from the boundary but also more closely to it. This fact is reflected in the lowering of the minimal value of the mean positions within a period. Notice that the two interacting particles will also attain more closely to each other.

In both cases depicted in Fig. 5.5 there are noticeable phase differences in the oscillations of mean positions. Nevertheless, the general relation

$$\tilde{\mu}_{\mathrm{L}}(t) + \tilde{\mu}_{\mathrm{R}}(t) = 2\tilde{\mu}(t) \tag{5.52}$$

holds for all times t. In terms of the differences between the mean positions this relation reads

$$\tilde{\mu}_{\mathrm{R}}(t) - \tilde{\mu}_{\mathrm{L}}(t) = 2\left[\tilde{\mu}(t) - \tilde{\mu}_{\mathrm{L}}(t)\right] \ . \tag{5.53}$$

Mean positions $\tilde{\mu}(t)$, $\tilde{\mu}_{\mathrm{L}}(t)$, and $\tilde{\mu}_{\mathrm{R}}(t)$ as the functions of time can not cross each other. The ordering of the mean positions $\tilde{\mu}_{\mathrm{R}}(t) > \tilde{\mu}(t) > \tilde{\mu}_{\mathrm{L}}(t)$ is conserved for all times t and all values of the parameters v_0, v_1, ω, and D.

5.2 Thermodynamics

Up to now, we have discussed *kinetic quantities*, i.e., the quantities directly related to the time- and space-dependence of the probability density. Presently, we will focus on the analysis of the underlying *thermodynamics*. Again, all the time we will consider the system already to get settled in the time-asymptotic stationary regime. First thermodynamic characteristic under investigation is the internal energy.

5.2.1 Internal energy

Let us again start with the equilibrium situation. As already mentioned, in the time-independent potential $\phi(x) = -xF_0$ the single diffusing particle approaches the equilibrium state described by the probability density (5.37). The system of two interacting particles approach the state with the marginal equilibrium densities (5.38), (5.39). The equilibrium internal energy of the particles is simply the spatial integral of the product of the potential energy and equilibrium probability density.[4] For the single diffusing particle the result is $E^{(\mathrm{eq})} = D\Gamma = k_{\mathrm{B}}T$. In the case of the diffusion of two interacting particles, the internal energy of the left particle reads $E_{\mathrm{L}}^{(\mathrm{eq})} = k_{\mathrm{B}}T/2$, the internal energy of the right one is $E_{\mathrm{R}}^{(\mathrm{eq})} = 3k_{\mathrm{B}}T/2$. Hence the equilibrium internal energies do not depend on the slope of the potential and linearly increase with the temperature. Moreover,

[4] Hence we do not care about contribution of the kinetic energy.

the total internal energy of the system of two interacting particles is equal to the total internal energy of the system of two non-interacting particles, i.e., $E_{\rm L}^{(\rm eq)}+E_{\rm R}^{(\rm eq)}=2E^{(\rm eq)}$. This fact emerges due to the zero range of the hard-core interaction, so the interaction induces purely geometric constraints on the possible positions of the particles. Hence the interaction energy is zero. This is a general feature of the hard-core interaction. As so its validity is not restricted only to the equilibrium case.

Returning to the time-dependent potential $\phi(x,t)=-xF(t)$, the internal energy of the particle at the time t is defined as potential averaged over all possible positions of the particle at a given instant (cf. Eq. (3.21)). In the single-particle case the internal energy of the particle at the time t reads

$$E(t)=\int_0^{+\infty}\mathrm{d}x\,\phi(x,t)\tilde{u}(x;t)=-[F_0+F_1\sin(\omega t)]\tilde{\mu}(t)\ . \tag{5.54}$$

Similarly, in the case with interaction, internal energies of the left and right particles are

$$E_{\rm L}(t)=-[F_0+F_1\sin(\omega t)]\tilde{\mu}_{\rm L}(t)\ , \tag{5.55}$$

$$E_{\rm R}(t)=-[F_0+F_1\sin(\omega t)]\tilde{\mu}_{\rm R}(t)\ , \tag{5.56}$$

respectively. Notice that we skip the tilde over the internal energies, although they are expressed in the asymptotic regime. In this Section all thermodynamic characteristics are considered in the asymptotic regime, hence the tilde is useless and will be omitted.

The mean positions occurred in the expressions above are given in Eq. (5.43), Eq. (5.46) and Eq. (5.47). As was mentioned above, in the thermodynamic equilibrium internal energies do not depend on the slope of the potential. Obviously, out of equilibrium this is not the case. However, the general rule "internal energy = mean position multiplied by the instantaneous force" holds in both equilibrium and non-equilibrium cases.[5]

Generally speaking, the internal energies $E(t)$, $E_{\rm L}(t)$, $E_{\rm R}(t)$ are periodic functions of time with the fundamental period $2\pi/\omega$. Their oscillations express the combine effect of both the periodically modulated heat flow to the bath and the periodic exchange of work done on the particle by an external agent. Moreover, from Eq. (5.52) it follows that the total internal energy of two interacting particles is equal to the total internal energy of two non-interacting particles. Couched in symbols

$$E_{\rm L}(t)+E_{\rm R}(t)=2E(t)\ . \tag{5.57}$$

In other words, the internal energy $E(t)$ of the single diffusing particle always equals to the arithmetic mean $(E_{\rm L}(t)+E_{\rm R}(t))/2$ of the internal energies of interacting particles.

[5]Due to the linearity of $\phi(x,t)$ in x.

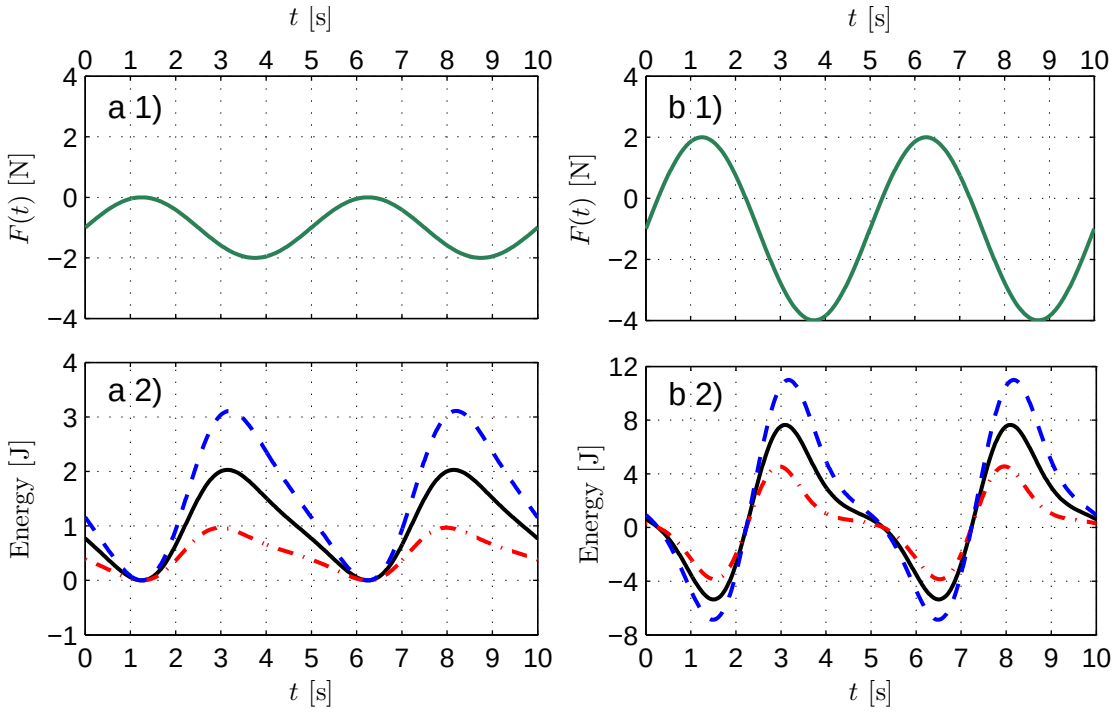

Figure 5.6: Oscillations of the internal energies within two periods of the driving. Two curves in the upper panels show the time-dependency of the driving force (5.2). Oscillations of the internal energies are shown in lower panels always bellow the corresponding driving force. The solid black line shows the energy $E(t)$, the dashed blue line depicts $E_{\mathrm{R}}(t)$ and the dot-dashed red line depicts $E_{\mathrm{L}}(t)$. In the panels a 1) and a 2) we take $F_1 = 1.0\,\mathrm{N}$, in the panels b 1) and b 2) we take $F_1 = 3.0\,\mathrm{N}$. The static component $F_0 = -1.0\,\mathrm{N}$, the frequency $\omega = 0.4\,\pi\,\mathrm{s}^{-1}$, and the diffusion constant $D = 1.0\,\mathrm{m}^2\mathrm{s}^{-1}$ are the same in all panels.

Fig. 5.6 shows the time-dependency of the internal energies $E(t)$, $E_{\mathrm{L}}(t)$, $E_{\mathrm{R}}(t)$ within two periods of the driving force for the different parameters F_0, F_1, ω, and D. The curves in the upper panels represent driving forces, the lower panels depict the induced oscillations of the internal energies (see the figure caption). The parameters used in this figure are the same as in Fig. 5.5. First of all, notice that there is no *qualitative* difference between the oscillations of the function $E(t)$ and the functions $E_{\mathrm{L}}(t)$, $E_{\mathrm{R}}(t)$. It the consequence of the fact that the hard-core interaction changes only *quantitative* features of the energetics of individual particles (as compared to the diffusion without interaction). One of this quantitative changes, the most striking one at first glance, is the change of the magnitudes of the internal energies. Whenever the force $F(t)$ is

negative it pushes particles against the boundary. In this case internal energies are ordered according to their magnitudes in the same way as their mean positions, i.e., $E_{\mathrm{R}}(t) > E(t) > E_{\mathrm{L}}(t)$. Hence the farther is the particle from the reflecting boundary, the greater is its internal energy. Whenever the driving force is zero, the internal energies are all equal. Positive driving force (cf. panels b 1), b 2)) pushes particles to the right, away from the boundary. In this case the ordering of the mean energies is reversed, i.e., $E_{\mathrm{L}}(t) > E(t) > E_{\mathrm{R}}(t)$ (while the ordering of the mean positions $\tilde{\mu}_{\mathrm{R}}(t) > \tilde{\mu}(t) > \tilde{\mu}_{\mathrm{L}}(t)$ is always the same). Notice also that the maximum values of the energies $E_{\mathrm{L}}(t)$, $E_{\mathrm{R}}(t)$ are achieved at the different instants within the period.

From a purely mathematical point of view the differences in the behaviour of the internal energies and the mean positions arise due to the multiplicative prefactor $-F(t)$ (see Eqs. (5.54) - (5.56)). However, the physical interpretation of the behaviour of the internal energies brings deeper insight into the problem. Without loss of generality let us concentrate on the case without the interaction, i.e. on the black lines in Fig. 5.6. As the beginning of the period we choose the instant when the driving force takes the value F_0 and tends to increase. It is increasing up to the value $F_0 + F_1$. In the panel a 2) $F_0 + F_1 = 0$ N, in the panel b 2) $F_0 + F_1 = 2$ N. During this interval the internal energy is decreasing towards its minimum due to the system is exerting positive work on its surrounding. The smaller is the value of the amplitude F_1 (panel a 2)) the closer is the process to the *quasistatic* one[6] and the smaller is the work done by the system. The decreasing tendency of the internal energy is being partially offset by the heat flow to the system from the heat bath. However, for larger amplitudes F_1 (panel b 2)) the heat is almost exclusively being released to the reservoir during this interval. So the greater is the amplitude F_1 the lower minimum values takes the internal energy within the period.

During the next time interval the driving force is decreasing form the value $F_0 + F_1$ to its minimum value $F_0 - F_1$. In the panel a 2) $F_0 - F_1 = -2$ N, in the panel b 2) $F_0 + F_1 = -4$ N. Within this interval the slop $-F(t)$ of the potential $\phi(x,t)$ is permanently rising, hence the positive work is performing on the system by an external agent. This work forms the most significant contribution to the changes of the internal energy which is rising and passing through its maximum within this interval. The decrease of the internal energy after it achieves its maximum value is caused by the strong heat flow from the system to the bath at occurred the end of this time-interval.

During the last part of the period the force and the internal energy are decreasing to their initial values which they take at the beginning of the period. Within this time-interval the slope of the potential $\phi(x,t)$ is decreasing, hence the work done by the system on its surrounding is positive. Notice the sudden change of the slope of the

[6]The quasistatic process is at all instants in the equilibrium with the heat bath.

time-dependency of the internal energy at the beginning of this interval. This change is more apparent for the greater amplitudes F_1 (panel b 2)). It is connected with the fact that the system starts to exert work on its surrounding. The greater is the amplitude F_1 the less significant is the contribution of this work to the change of an internal energy as compared with the heat flow from the system to the reservoir (more significant contribution of the work would cause faster decreasing of the internal energy as should be seen from panel a 2)).

We have just observed how the amplitude F_1 of the modulated force influences the behaviour of the oscillations of the internal energy. The amplitudes of these oscillations rise and the oscillations became more *nonlinear* as the amplitude F_1 increases. In the following sections we give a detailed discussion of the underlying exchange of work and heat. So we recommend to the reader to get back to the presented discussion again after reading the corresponding Subsections to get even more insight into the energetics of the problem.

Finally let us discus the internal energies averaged over the period

$$\bar{E} = \frac{\omega}{2\pi}\int_0^{2\pi/\omega} \mathrm{d}t E(t) \ , \tag{5.58}$$

$$\bar{E}_{\mathrm{L}} = \frac{\omega}{2\pi}\int_0^{2\pi/\omega} \mathrm{d}t E_{\mathrm{L}}(t) \ , \tag{5.59}$$

$$\bar{E}_{\mathrm{R}} = \frac{\omega}{2\pi}\int_0^{2\pi/\omega} \mathrm{d}t E_{\mathrm{R}}(t) \ . \tag{5.60}$$

This quantities are obviously controlled by the zero Fourier coefficients μ_0, λ_0, ρ_0 from the Fourier series representations of the mean positions (5.43), (5.46) and (5.47). We have $\bar{E} = -F_0\mu_0$, $\bar{E}_{\mathrm{L}} = -F_0\lambda_0$, $\bar{E}_{\mathrm{R}} = -F_0\rho_0$. Hence all comments made about the stationary mean positions μ_0, λ_0, and ρ_0 in the preceding Subsection could be directly applied to the internal energies averaged over the period. Notice that the differences $\bar{E} - E^{(\mathrm{eq})}$, $\bar{E}_{\mathrm{L}} - E_{\mathrm{L}}^{(\mathrm{eq})}$, and $\bar{E}_{\mathrm{R}} - E_{\mathrm{R}}^{(\mathrm{eq})}$ are always greater than zero. Differently speaking, in the time-averaged sense, the external driving enforces a *permanent increase of the internal energy* of particles as compared to its equilibrium value. This is true for both the interacting particles and the single diffusing particles.

5.2.2 Work

The average work done on the single diffusing particle by an external agent during the time interval $[0, t]$ reads (cf. Eq. (3.23))

$$W(t) = \int_0^t \mathrm{d}t' \int_{-\infty}^{+\infty} \mathrm{d}x \left[\frac{\partial}{\partial t'}\phi(x, t')\right] \tilde{u}(x; t') = -F_1\omega \int_0^t \mathrm{d}t' \cos(\omega t')\tilde{\mu}(t') \ . \tag{5.61}$$

Similarly, in the case with the interaction, the average work done on the left and on the right particle the time interval $[0, t]$ reads

$$W_{\mathrm{L}}(t) = -F_1\omega \int_0^t \mathrm{d}t' \cos(\omega t')\tilde{\mu}_{\mathrm{L}}(t') \ , \tag{5.62}$$

$$W_{\mathrm{R}}(t) = -F_1\omega \int_0^t \mathrm{d}t' \cos(\omega t')\tilde{\mu}_{\mathrm{R}}(t') \tag{5.63}$$

respectively. Hence the average work[7] done on the system equals the area enclosed by the hysteresis curve which represents the parametric plot of the negative taken oscillating force $-F_1 \sin(\omega t)$ versus the mean coordinate.

Work done on the system during a definite time interval within the period can be both positive and negative. It could be negative when the slope of the potential decreases. Otherwise it is positive. Its actual value depends on the localisation of the particles, within a given time-interval. The absolute value of the work is bigger if the particles are farther from the boundary. The hard-core interaction in average shifts the right (left) tagged particle to the right (left) as compared to the case without interaction. Hence the absolute value of work done on the right (left) particle is bigger (smaller) than in the case without interaction. In spite of this, the total work done on the system of two interacting particles equals to the total work done on two non-interacting particles[8], i.e., we have

$$W_{\mathrm{L}}(t) + W_{\mathrm{R}}(t) = 2W(t) \ . \tag{5.64}$$

All these properties are illustrated in Fig. 5.7. It shows works $W(t)$, $W_{\mathrm{L}}(t)$, $W_{\mathrm{R}}(t)$ as the functions of the interval length t within two periods of the driving force for the different parameters (also used in Fig. 5.5 and Fig. 5.6). In addition to the already mentioned properties notice three another important features of depicted works. First apparent feature is that there are no *qualitative* differences between the depicted oscillations of the work $W(t)$ and the works $W_{\mathrm{L}}(t)$, $W_{\mathrm{R}}(t)$. These oscillations differ only in their amplitudes (obviously due to the hard-core interaction). The works $W(t)$, $W_{\mathrm{L}}(t)$ and $W_{\mathrm{R}}(t)$ are *not* periodic functions of the interval length t (the period $2\pi/\omega$ lasts 5 s in Fig. 5.7). The value achieved by $W(t)$ at the end of the period minus its value at the beginning of the period is equal to the work done on the single-diffusing particle by an external agent per one period. The same is true for interacting particles. The work done on the system per period must be always non-negative. Otherwise, the system in contact with the single heat bath at one fixed temperature would produce positive work during the cyclic process. Analytical results for the work per period are derived and

[7] Further, we will omit the word "average" and write only "work".

[8] Introduce Eq. (5.52) into Eq. (5.61) for a proof.

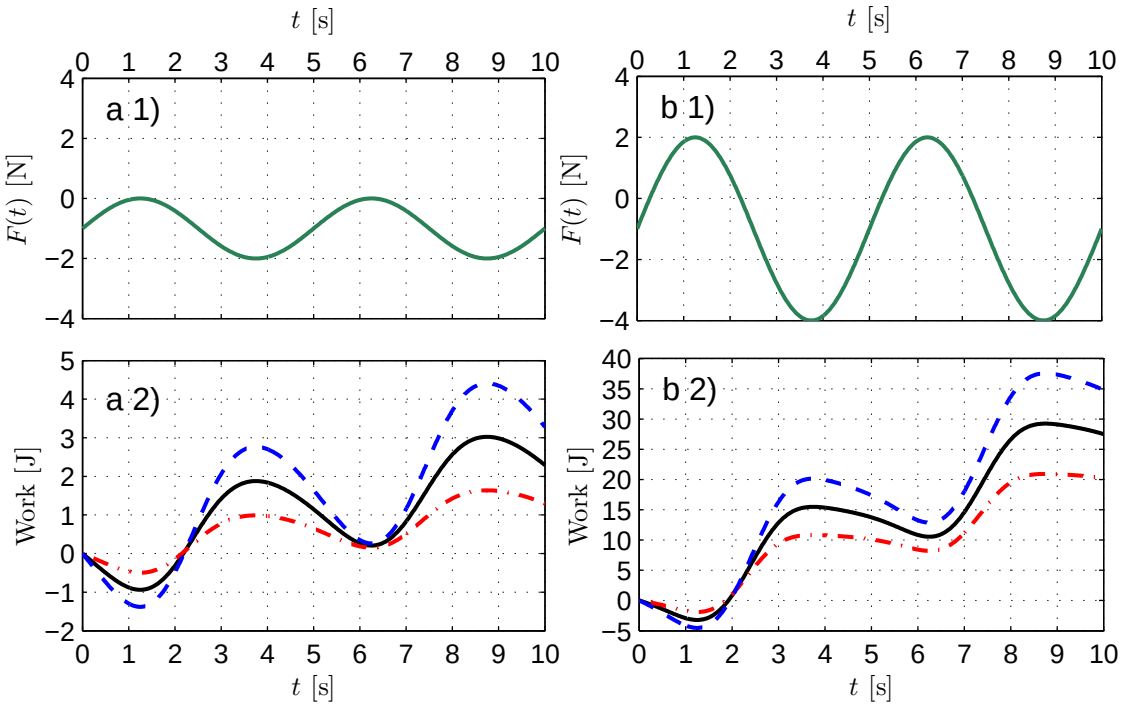

Figure 5.7: Work done on the system by the external agent during the time interval $[0, t]$ as the function of the interval length t. The curves in the upper panels show the time-dependency of the driving force (5.2). The work as the function of the interval length t is shown in the lower panels always bellow the corresponding driving force. The solid black line shows the function $W(t)$, the dashed blue line depicts $W_{\mathrm{R}}(t)$ and the dot-dashed red line depicts $W_{\mathrm{L}}(t)$. In the panels a 1) and a 2) we take $F_1 = 1.0\,\mathrm{N}$, in the panels b 1) and b 2) we take $F_1 = 3.0\,\mathrm{N}$. The static component $F_0 = -1.0\,\mathrm{N}$, the frequency $\omega = 0.4\,\pi\,\mathrm{s}^{-1}$, and the diffusion constant $D = 1.0\,\mathrm{m}^2\mathrm{s}^{-1}$ are the same in all panels.

more closely discussed below. Finally, notice the differences in the relative contributions to work per period between the increasing and the decreasing part of depicted works $W(t)$, $W_{\mathrm{L}}(t)$ and $W_{\mathrm{R}}(t)$. This relative contributions apparently differ for the different parameters. The bigger is the amplitude F_1 of the oscillating force, the less relevant are the relative contributions of decreasing parts of the depicted works. Hence the farther is the system from the thermodynamic equilibrium the relatively less useful work it produces. On the other hand, the smaller is the amplitude F_1 the smaller is the work per period, hence the smaller is the absolute useful work (work done by the system on its surrounding during the period). In the limit of the quasistatic process work per

period is zero, i.e., the overall work done on the system equals to the work done by the system at the end of the period. For the quasistatic process the relative values of the work done on the system and by the system are equal and the latter is the maximal possible. This observation is crucial for an understanding of the time dependency of the internal energies.

We now study the work done on the system per one period. Let $W^{(\mathrm{per})}$ denote this work done on the single diffusing particle. Then we have

$$W^{(\mathrm{per})} \equiv W(2\pi/\omega) = -F_1\omega \int_0^{2\pi/\omega} \mathrm{d}t' \cos(\omega t')\tilde{\mu}(t') \ . \tag{5.65}$$

Using the Fourier series representation (5.43) of the mean position $\tilde{\mu}(t)$ we can rewrite Eq. (5.65) in the form

$$W^{(\mathrm{per})} = -F_1\omega \sum_{k=-\infty}^{+\infty} \mu_k \int_0^{2\pi/\omega} \mathrm{d}t' \cos(\omega t') \exp(-\mathrm{i}k\omega t') \ . \tag{5.66}$$

Since $\exp(-\mathrm{i}k\omega t) = \cos(k\omega t) - \mathrm{i}\sin(k\omega t)$ and the sine and cosine functions are orthogonal, only two terms from the summation will survive the integration in Eq. (5.66). Thus

$$W^{(\mathrm{per})} = -F_1\pi\left(\mu_1 + \mu_{-1}\right) = -2\pi F_1 \mathrm{Re}\,\mu_1 \ , \tag{5.67}$$

where the first Fourier coefficient μ_1 is given by Eq. (5.44).

In the completely similar way we obtain works per period performed on the interacting particles. Let $W_{\mathrm{L}}^{(\mathrm{per})}$ ($W_{\mathrm{R}}^{(\mathrm{per})}$) denote this work done on the left (right) particle, then we have

$$W_{\mathrm{L}}^{(\mathrm{per})} = -2\pi F_1 \mathrm{Re}\,\lambda_1 \ , \tag{5.68}$$

$$W_{\mathrm{R}}^{(\mathrm{per})} = -2\pi F_1 \mathrm{Re}\,\rho_1 \ , \tag{5.69}$$

where the first Fourier coefficients λ_1, ρ_1 are given by Eq. (5.48), Eq. (5.49).

As was mentioned above, the works per period $W^{(\mathrm{per})}$, $W_{\mathrm{L}}^{(\mathrm{per})}$, $W_{\mathrm{R}}^{(\mathrm{per})}$ are *always non-negative*. Therefore the real parts of the first Fourier coefficients μ_1, λ_1 and ρ_1 must always have the opposite sign than the amplitude F_1. Up to the multiplicative factor $D/|v_0|$, the first Fourier coefficients depends solely on the parameter combinations $\zeta = 4\omega D/v_0^2$ and $\kappa = |v_0|v_1/(2\omega D)$. Hence their real parts have to be odd functions of the parameter κ.

Two relations

$$\begin{aligned} W_{\mathrm{L}}^{(\mathrm{per})} + W_{\mathrm{R}}^{(\mathrm{per})} &= 2W^{(\mathrm{per})} \ , \\ W_{\mathrm{L}}^{(\mathrm{per})} < W^{(\mathrm{per})} &< W_{\mathrm{R}}^{(\mathrm{per})} \ , \end{aligned} \tag{5.70}$$

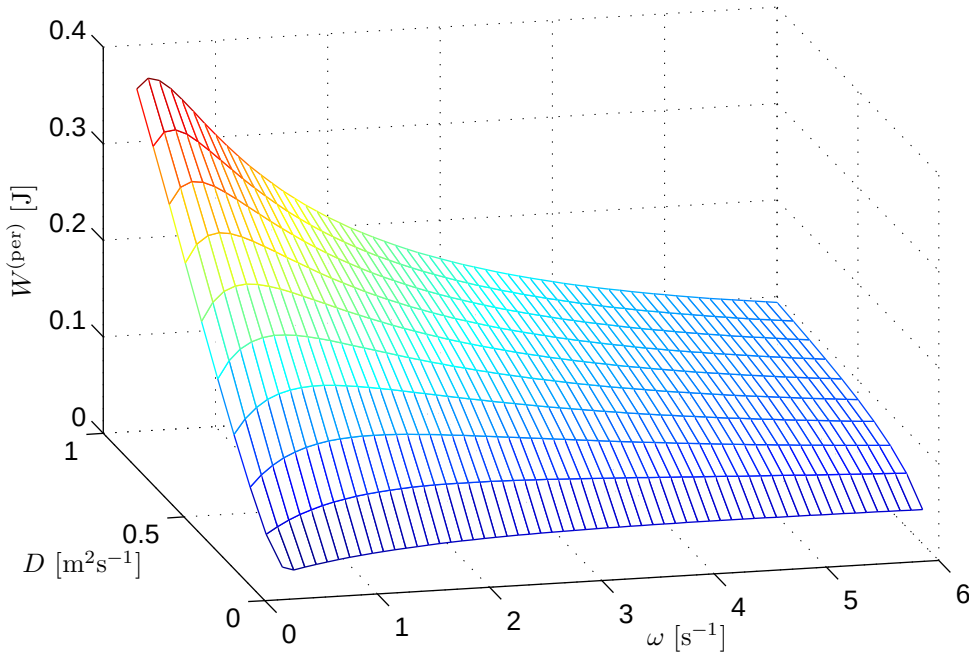

Figure 5.8: Work done on the single-diffusing particle per one period of the driving as the function of the frequency ω and the heat bath temperature represented by the diffusion constant D. As usual in this thesis we have taken $\Gamma = 1.0\,\mathrm{kg\,s^{-1}}$, $k_\mathrm{B} = 1.0\,\mathrm{J\,K^{-1}}$, hence the diffusion constant D is numerically equal to the heat bath temperature. The amplitudes of the driving force are $F_0 = -1.0\,\mathrm{N}$, $F_1 = 0.5\,\mathrm{N}$.

hold for any values of the parameters F_0, F_1, ω, and D. The first one is nothing but Eq. (5.64) for $t = 2\pi/\omega$. The second follows from the first one and the observation that the absolute value of work is always bigger if the particle is farther from the boundary.

The works per period $W^{(\mathrm{per})}$, $W_\mathrm{L}^{(\mathrm{per})}$ and $W_\mathrm{R}^{(\mathrm{per})}$ behave qualitatively in the same way as the functions of the parameters F_0, F_1, ω, and D. Hence in the following we restrict our discussion to one of them, namely to the function $W^{(\mathrm{per})}$.

From the numerical analysis we know that the work $W^{(\mathrm{per})}$ is a monotonic convex increasing function of the amplitudes F_0, F_1 (the figure which illustrates this fact is not very interesting and is not presented here). It is a monotonic concave increasing function of temperature as represented by the diffusion constant D and exhibits the maximum as the function of frequency ω. Last two facts are illustrated in Fig. 5.8. Notice that the maximum shifts towards the lower frequencies (i.e., longer periods) and became more

pronounced as temperature of the heat bath increases. Work $W^{(\mathrm{per})}$ is nothing but the amount of energy irretrievably dissipated in form of heat released to the bath per one period. This dissipation (or *irretrievable absorption* of energy) is maximal for a certain frequency ω. The maximum amount of absorbed energy depends on temperature of the bath (for fixed amplitudes F_0, F_1).

All statements made about $W^{(\mathrm{per})}$ are also valid for $W_{\mathrm{L}}^{(\mathrm{per})}$ and $W_{\mathrm{R}}^{(\mathrm{per})}$. This functions are also convex increasing functions of F_0, F_1, concave increasing functions of D and exhibit maxima as the functions of the frequency ω. However, this maxima occur at a slightly different frequencies[9].

5.2.3 Heat

Heat is the form of energy transfer between the system and the heat bath realized in any other way than due to work performed on the system [66]. Any other way means by the changes of the "occupation probabilities" of the "energy levels" of the system. Of course in our case the energy spectrum (given by the potential $\phi(x,t)$) is continuous and the "occupation probabilities" are represented by the probability density for the position of the particle.

Let us first consider the single-particle case. The heat released to the heat bath during the infinitesimal time interval $(t, t+\mathrm{d}t)$ according to Eq. (3.22) reads

$$\mathrm{d}Q(t) = \mathrm{d}t\, F(t) \int_0^{+\infty} \mathrm{d}x\, \tilde{J}(x;t) \ , \tag{5.71}$$

where

$$\tilde{J}(x;t) = \left[\frac{F(t)}{\Gamma} - D\frac{\partial}{\partial x} \right] \tilde{u}(x;t) \ , \tag{5.72}$$

denotes the probability current in the time-asymptotic regime. Performing the integration we arrive at the expression

$$\mathrm{d}Q(t) = \mathrm{d}t\, \frac{F(t)}{\Gamma} \left[F(t) + k_{\mathrm{B}}T\, \tilde{u}(0;t) \right] \ . \tag{5.73}$$

There are two parts of the *integrated current* $\int_0^{+\infty} \mathrm{d}x\, \tilde{J}(x;t)$ left in the square brackets on the right-hand side of Eq. (5.73). The first is the *drift* part, the second is the *diffusive*. The latter contain the thermal energy $k_{\mathrm{B}}T$ multiplied by the probability density at the boundary (5.15). An interplay of this two currents determines the sign of the heat flow

[9] We discuss this more closely in Subsec. 5.2.4 (Fig. 5.10).

$\mathrm{d}Q(t)$. Obviously it could be both, positive and negative depending on the values of the parameters.

Moreover, the integration by parts of the time-derivative of the mean position gives the relation

$$\frac{\mathrm{d}}{\mathrm{d}t}\tilde{\mu}(t) = \int_0^{+\infty} \mathrm{d}x\, \tilde{J}(x;t) \ . \tag{5.74}$$

Eq. (5.74) together with Eq. (5.71) establish the relationship between the heat flow and the change of the particle's mean position. From Eq. (5.71) we obtain

$$\mathrm{d}Q(t) = F(t)\, \mathrm{d}\tilde{\mu}(t) \ . \tag{5.75}$$

Similar relations hold also for a tagged particles, i.e.,

$$\mathrm{d}Q_{\mathrm{L}}(t) = F(t)\, \mathrm{d}\tilde{\mu}_{\mathrm{L}}(t) \ , \tag{5.76}$$

$$\mathrm{d}Q_{\mathrm{R}}(t) = F(t)\, \mathrm{d}\tilde{\mu}_{\mathrm{R}}(t) \ , \tag{5.77}$$

where $\mathrm{d}Q_{\mathrm{L}}(t)$ ($\mathrm{d}Q_{\mathrm{R}}(t)$) is the amount of heat released to the reservoir during the time interval $(t, t+\mathrm{d}t)$ by the left (right) particle.

Thus *the necessary and sufficient condition for an energy transfer in the form of heat between the system and the bath is a motion of the particle in an averaged sense under the action of a non-zero force.*

Heat released to the heat bath within the time interval $[0, t]$ in the single-particle case, by the left particle, by the right particle reads

$$Q(t) = [F(t)\tilde{\mu}(t) - F(0)\tilde{\mu}(0)] - F_1\omega \int_0^t \mathrm{d}t' \cos(\omega t')\tilde{\mu}(t') \ , \tag{5.78}$$

$$Q_{\mathrm{L}}(t) = [F(t)\tilde{\mu}_{\mathrm{L}}(t) - F(0)\tilde{\mu}_{\mathrm{L}}(0)] - F_1\omega \int_0^t \mathrm{d}t' \cos(\omega t')\tilde{\mu}_{\mathrm{L}}(t') \ , \tag{5.79}$$

$$Q_{\mathrm{R}}(t) = [F(t)\tilde{\mu}_{\mathrm{R}}(t) - F(0)\tilde{\mu}_{\mathrm{R}}(0)] - F_1\omega \int_0^t \mathrm{d}t' \cos(\omega t')\tilde{\mu}_{\mathrm{R}}(t') \ , \tag{5.80}$$

respectively. The first term on the right-hand sides is nothing but the change of the internal energy. The second term is the work performed on the corresponding particle during the time interval $[0, t]$. The functions $Q(t)$, $Q_{\mathrm{L}}(t)$, and $Q_{\mathrm{R}}(t)$ are illustrated in Fig. 5.9 as the functions of the interval length t for different values of the parameters (also used in Fig. 5.6 and Fig. 5.7).

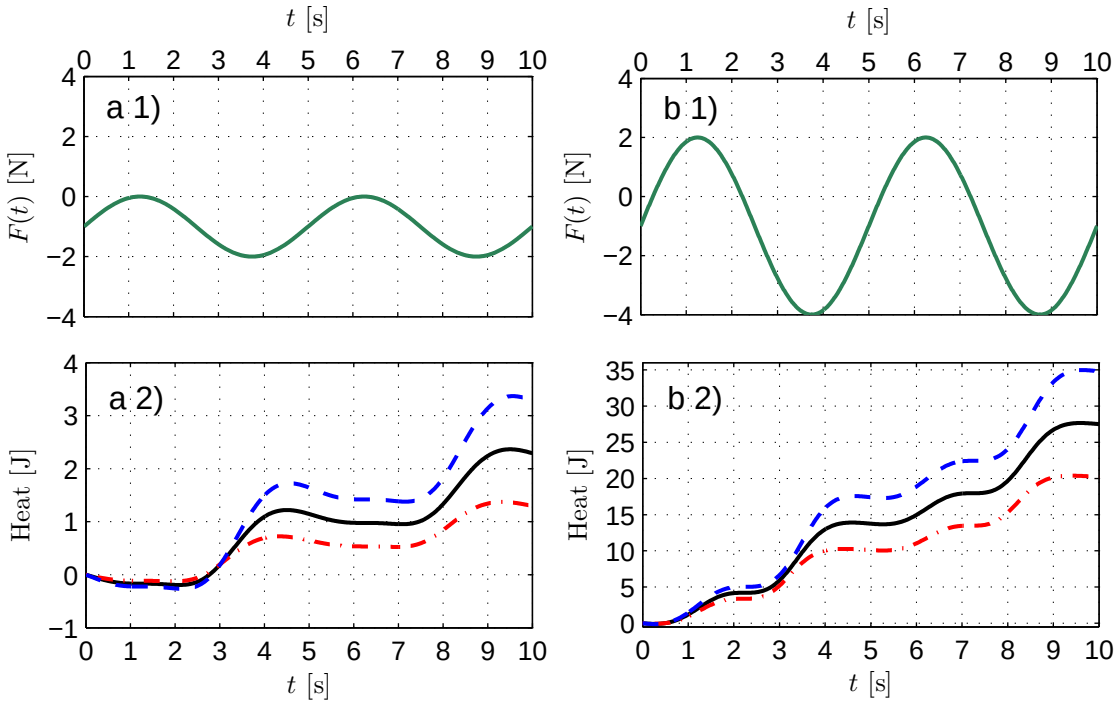

Figure 5.9: Heat released to the heat bath during the time interval $[0, t]$ as the function of the interval length t. The curves in the upper panels show the time-dependency of the driving force (5.2). The heat released to the heat bath during the time interval $[0, t]$ as the function of the interval length t is shown in the lower panels always bellow the corresponding driving force. The solid black line depicts the function $Q(t)$, the dashed blue line depicts $Q_{\mathrm{R}}(t)$ and the dot-dashed red line depicts $Q_{\mathrm{L}}(t)$. In the panels a 1) and a 2) we take $F_1 = 1.0\,\mathrm{N}$, in the panels b 1) and b 2) we take $F_1 = 3.0\,\mathrm{N}$. The static component $F_0 = -1.0\,\mathrm{N}$, the frequency $\omega = 0.4\,\pi\,\mathrm{s}^{-1}$, and the diffusion constant $D = 1.0\,\mathrm{m}^2\mathrm{s}^{-1}$ are the same in all panels.

Having periodic changes of the internal energy, the heat dissipated during one period is equal to the work done on the system during one period. We have

$$Q^{(\mathrm{per})} \equiv Q(2\pi/\omega) = W^{(\mathrm{per})} , \tag{5.81}$$

$$Q_{\mathrm{L}}^{(\mathrm{per})} \equiv Q_{\mathrm{L}}(2\pi/\omega) = W_{\mathrm{L}}^{(\mathrm{per})} , \tag{5.82}$$

$$Q_{\mathrm{R}}^{(\mathrm{per})} \equiv Q_{\mathrm{L}}(2\pi/\omega) = W_{\mathrm{R}}^{(\mathrm{per})} . \tag{5.83}$$

The work per period has been discussed at the end of Subsec. 5.2.2.

5.2.4 Entropy

In the previous Subsection, we have introduced the heats $Q(t)$, $Q_{\rm L}(t)$, $Q_{\rm R}(t)$ released to the heat bath within the time interval $[0,t]$ by the individual particles. Since the heat bath is kept at constant temperature T, the entropy change of the bath during the time-interval $[0,t]$ is

$$S(t) = \frac{Q(t)}{T} \tag{5.84}$$

in the case of the single diffusing particle. During the diffusion with interaction, the left particle increases the entropy of the heat bath by

$$S_{\rm L}(t) = \frac{Q_{\rm L}(t)}{T} \ , \tag{5.85}$$

the right particle by

$$S_{\rm R}(t) = \frac{Q_{\rm R}(t)}{T} \ . \tag{5.86}$$

The contributions (5.85) and (5.86) give the total entropy produced in the heat bath. Moreover, the total change of the heat bath entropy in the case with interactions equals to $2S(t)$, i.e., it is the same as for two non-interacting particles.

The heats $Q(t)$, $Q_{\rm L}(t)$, and $Q_{\rm R}(t)$ as the functions of the interval length t are depicted in Fig. 5.9. In this figure the heats are numerically equal to the entropy productions (5.84), (5.85), and (5.86).

We now consider the entropy produced during one period. The entropy of the system (be it the single diffusing particle, or the two interacting particles) is a periodic function with the period $2\pi/\omega$. Hence the *total* entropy produced during the period is equal to the heat released to the heat bath during one period divided by the temperature of the heat bath. For the single diffusing particle the total entropy production per one period reads

$$S^{(\rm per)} \equiv \frac{Q^{(\rm per)}}{T} = \frac{W^{(\rm per)}}{T} = -2\pi k_{\rm B} \frac{v_1}{D} {\rm Re}\, \mu_1 \ , \tag{5.87}$$

where the equality between $Q^{(\rm per)}$ and $W^{(\rm per)}$ holds due to the periodicity of the internal energy. In addition, we have used Eq. (5.67) and relations $T = \Gamma D/k_{\rm B}$, $v_1 = F_1/\Gamma$. Similarly, for the diffusion with the interaction the total entropy produced by the left, right particle reads

$$S_{\rm L}^{(\rm per)} \equiv \frac{Q_{\rm L}^{(\rm per)}}{T} = -2\pi k_{\rm B} \frac{v_1}{D} {\rm Re}\, \lambda_1 \ , \tag{5.88}$$

$$S_{\rm R}^{(\rm per)} \equiv \frac{Q_{\rm R}^{(\rm per)}}{T} = -2\pi k_{\rm B} \frac{v_1}{D} {\rm Re}\, \rho_1 \ , \tag{5.89}$$

respectively (cf. Eq. (5.68) and Eq. (5.69)). The entropies $S_{\mathrm{L}}^{(\mathrm{per})}$ and $S_{\mathrm{R}}^{(\mathrm{per})}$ are additive, i.e., the total entropy produced by the system consisted of two interacting particles equals to the sum of entropies produced by the individual particles.

Expressions (5.87), (5.88), (5.89) represents the *exact analytical* formulae for entropy productions per one period. Now we determine their behaviour in dependence of the parameters F_0, F_1, ω, and D. Let us start with the single-particle case. At the end of Subsec. 5.2.2 we have shown that the work $W^{(\mathrm{per})}$ is the concave increasing function of temperature T and it exhibits maximum as the functions of frequency ω. After dividing this function by the bath temperature (cf. Eq. (5.87)) we obtain the entropy production $S^{(\mathrm{per})}$, which is *symmetric under the change of parameters ω and D*. Indeed, if we take $k = 1$ in Eq. (5.44) and insert μ_1 into Eq. (5.87), we get

$$S^{(\mathrm{per})} = -2\pi k_{\mathrm{B}} \frac{v_1}{|v_0|} \mathrm{Re}\, \langle 1 \,|\, \mathbb{L}_{--} \mathbb{K}\, \mathbb{R}_{++} \,|\, f \rangle \ , \tag{5.90}$$

where the expression $\langle 1 \,|\, \mathbb{L}_{--} \mathbb{K}\, \mathbb{R}_{++} \,|\, f \rangle$ depends solely on the parameter combinations $\zeta = 4\omega D / v_0^2$ and $\kappa = |v_0| v_1 / (2\omega D)$. The same reasoning remains valid also in the case with interaction. The entropy productions $S_{\mathrm{L}}^{(\mathrm{per})}$ and $S_{\mathrm{R}}^{(\mathrm{per})}$ are also symmetric under the change of ω and D (however, we have not found any simple expression for these functions). Hence *the heat bath temperature and the frequency are in a certain manner mutually interchangeable concerning the entropy production.*

The entropy productions $S^{(\mathrm{per})}$, $S_{\mathrm{L}}^{(\mathrm{per})}$ and $S_{\mathrm{R}}^{(\mathrm{per})}$ as the functions of heat bath temperature T represented by the diffusion constant D and frequency ω are illustrated in Fig. 5.10. Notice that all depicted functions qualitatively do not differ from one another. They seem to be only differently scaled. It is the demonstration of the fact that the hard-core interaction does not introduce any new qualitative features into the behaviour of the total entropy production. Each depicted function ($S^{(\mathrm{per})}$, $S_{\mathrm{L}}^{(\mathrm{per})}$ or $S_{\mathrm{R}}^{(\mathrm{per})}$) exhibits maximum as the function of the temperature (frequency), while other parameters are kept fixed. However, those maxima are placed at a slightly different temperatures (frequencies). For $S_{\mathrm{L}}^{(\mathrm{per})}$ it is shifted towards the highest temperatures (frequencies) as compared with $S_{\mathrm{R}}^{(\mathrm{per})}$. The maximum of the function $S^{(\mathrm{per})}$ is always located in a temperature (frequency) range between the maxima of $S_{\mathrm{R}}^{(\mathrm{per})}$ and $S_{\mathrm{L}}^{(\mathrm{per})}$ due to the (omnipresent) property $S^{(\mathrm{per})} = (S_{\mathrm{L}}^{(\mathrm{per})} + S_{\mathrm{R}}^{(\mathrm{per})})/2$.

The aforementioned behaviour of the entropy production per one period in dependence on the heat bath temperature and frequency (see Fig. 5.10) could be intuitively understood as follows. For large frequencies the over-damped system is not able to follow the driving force. Therefore, for infinitely large frequencies the influence of the driving force on the state of the system vanishes. As well do the heat exchanged between the system and heat bath per one period, hence the entropy production vanishes.

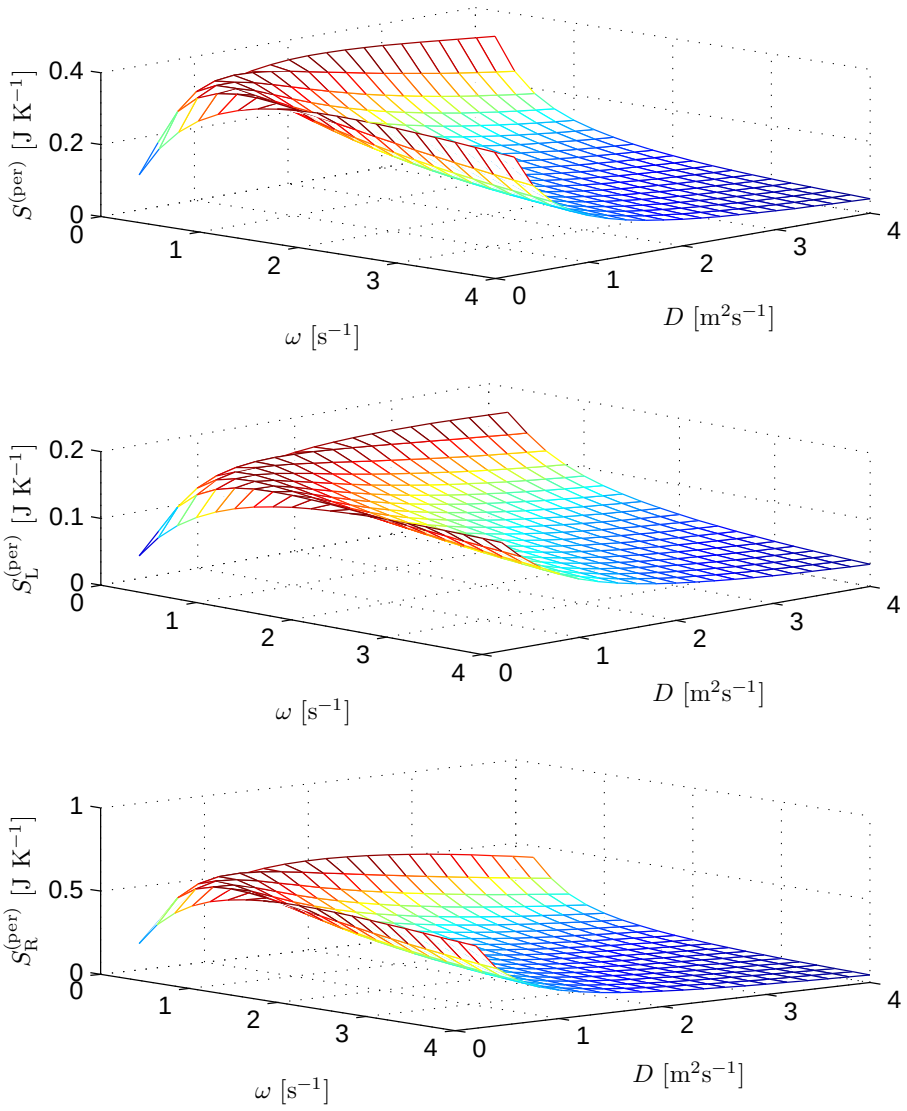

Figure 5.10: Entropy productions per one period as the functions of the frequency $\omega \in [0.2, 4.0]\,\mathrm{s}^{-1}$ and the diffusion constant $D \in [0.2, 4.0]\,\mathrm{m}^2\mathrm{s}^{-1}$. We have taken $F_0 = -1.0\,\mathrm{N}$, $F_1 = 0.5\,\mathrm{N}$, $\Gamma = 1.0\,\mathrm{kg\,s}^{-1}$, and $k_{\mathrm{B}} = 1.0\,\mathrm{J\,K}^{-1}$, hence the diffusion constant D is numerically equal to the heat bath temperature T.

On the other hand, the lower is the frequency, the "more reversible" is the diffusion process. For an infinitesimally small frequency, the system is at all times in a thermal equilibrium with the heat bath and, of course, such a process does not increase the total entropy. Moreover, in the limit of zero frequency no oscillations of the driving force occur.

Temperature dependence of the entropy production is *of quite a different nature* than its dependency on the frequency of the driving force. All the more remarkable are the symmetries of the functions $S^{(\mathrm{per})}$, $S_{\mathrm{L}}^{(\mathrm{per})}$ and $S_{\mathrm{R}}^{(\mathrm{per})}$ under the change of D and ω. The heat bath temperature determines the *thermal noise strength*. As such, it directly influences the spatial broadness of the probability densities of the particles' coordinates. In the limit of very low temperature, the thermal noise strength tends to zero, hence we obtain a *deterministic* motion of the particles. No heat is exchanged during one period of such a motion, therefore the entropy production tends to zero as the temperature is lowered. If the temperature is large enough, the probability densities will be spread over the wide range of the half-line $x \in [0, +\infty]$ apart from driving force. Consequently, time-dependent force does not affect the probability densities as well as the mean positions of the particles. Therefore again no heat will be transferred between the system and the heat bath (cf. Eq. (5.75), Eq. (5.76) and Eq. (5.77)) during a period and also no new entropy will be created.

Although intuitively plausible, to be well-founded the arguments presented above demand asymptotic expansions of the first Fourier coefficients in Eq. (5.87), Eq. (5.88), Eq. (5.89). We do not proceed in that way. Rather we now consider the *instantaneous* entropy of the system.

For the single-diffusing particle we define the instantaneous entropy as

$$H(t) = -k_{\mathrm{B}} \int_0^{+\infty} \mathrm{d}x \, \tilde{u}(x;t) \log \tilde{u}(x;t) \ . \tag{5.91}$$

Similarly, in the case with the interaction, the entropies of the left and right particles at time t read

$$H_{\mathrm{L}}(t) = -k_{\mathrm{B}} \int_0^{+\infty} \mathrm{d}x \, \tilde{p}_{\mathrm{L}}(x;t) \log \tilde{p}_{\mathrm{L}}(x;t) \ , \tag{5.92}$$

$$H_{\mathrm{R}}(t) = -k_{\mathrm{B}} \int_0^{+\infty} \mathrm{d}x \, \tilde{p}_{\mathrm{R}}(x;t) \log \tilde{p}_{\mathrm{R}}(x;t) \ , \tag{5.93}$$

respectively.[10] The entropies $H(t)$, $H_{\mathrm{L}}(t)$, and $H_{\mathrm{R}}(t)$ as the functions of time t are illustrated in Fig. 5.11, as usually, for two different values of the parameters (also used in Fig. 5.6, Fig. 5.7 and Fig. 5.9). Notice that in comparison with the mean values

[10] log denotes a logarithm to the base e.

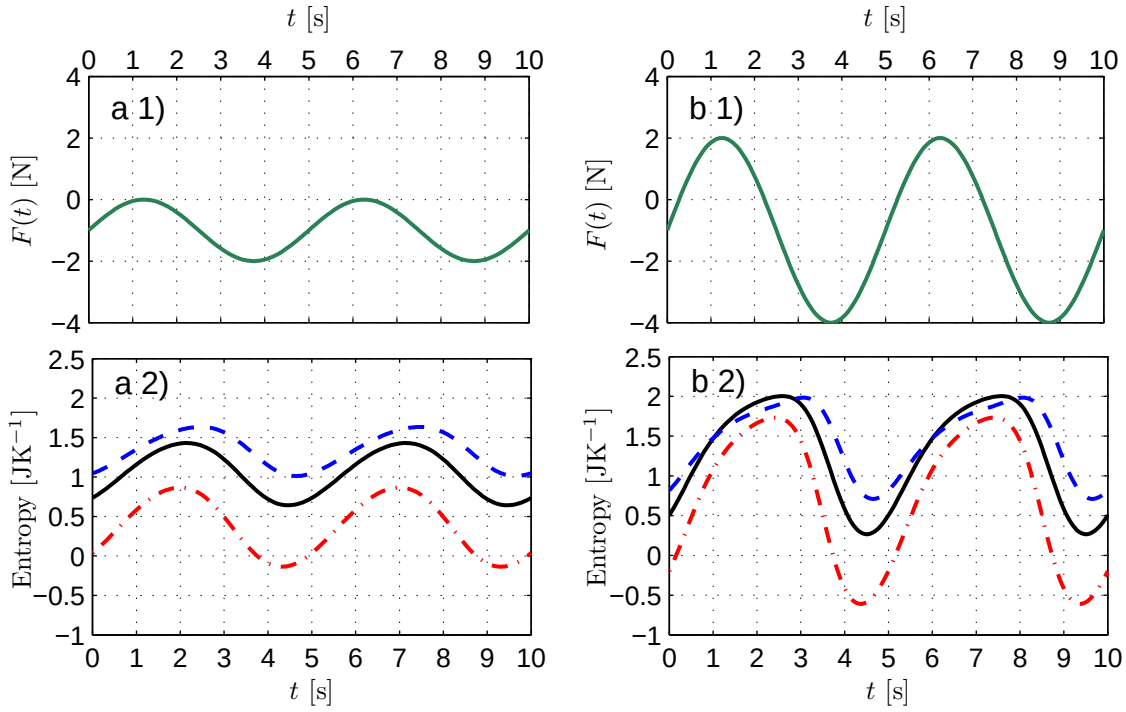

Figure 5.11: Entropies $H(t)$ (the solid black line), $H_{\mathrm{L}}(t)$ (the dashed blue line) and $H_{\mathrm{R}}(t)$ (the dot-dashed red line) as the functions time. The curves in the upper panels show the time-dependency of the driving force (5.2). In the panels a 1) and a 2) we take $F_1 = 1.0\,\mathrm{N}$, in the panels b 1) and b 2) we take $F_1 = 3.0\,\mathrm{N}$. The common parameters for all panels read $F_0 = -1.0\,\mathrm{N}$, $\omega = 0.4\,\pi\,\mathrm{s}^{-1}$, and $D = 1.0\,\mathrm{m}^2\mathrm{s}^{-1}$.

and all energetic quantities (internal energy, heat and work), the entropies lack one omnipresent property. *They are not additive*. Really, if we define the *joint entropy* for the system of two interacting particles as

$$H^{(2)}(t) = -k_{\mathrm{B}} \int_0^{+\infty} \mathrm{d}x_1 \int_0^{+\infty} \mathrm{d}x_2\, \tilde{p}^{(2)}(x_1, x_2; t) \log \tilde{p}^{(2)}(x_1, x_2; t) \;, \tag{5.94}$$

then it is easy to see (using Eq. (5.19)) that $H^{(2)}(t) = 2H(t)$, but $H_{\mathrm{L}}(t) + H_{\mathrm{R}}(t) \neq H^{(2)}(t)$, thus $H_{\mathrm{L}}(t) + H_{\mathrm{R}}(t) \neq 2H(t)$. Moreover, the inequality

$$H_{\mathrm{L}}(t) + H_{\mathrm{R}}(t) < 2H(t) \;, \tag{5.95}$$

holds for all times t.

A remarkable quantity possessed of interesting interpretation is a difference

$$\Delta H(t) \equiv 2H(t) - [H_{\mathrm{L}}(t) + H_{\mathrm{R}}(t)] \ . \tag{5.96}$$

Using the relation $\tilde{p}_{\mathrm{L}}(x;t)+\tilde{p}_{\mathrm{R}}(x;t) = 2\tilde{u}(x;t)$ (cf. Eq. (5.11)) and a few purely algebraic manipulations we convert Eq. (5.96) into the form

$$\Delta H(t) = k_{\mathrm{B}} K[\tilde{p}_{\mathrm{L}}, \tilde{u}] + k_{\mathrm{B}} K[\tilde{p}_{\mathrm{R}}, \tilde{u}] \ , \tag{5.97}$$

where $K[p,q]$ denotes the *Kullback-Leiber distance* between the probability densities p and q (cf. Eq. (3.26)). As was mentioned in Sec 3.4, the Kullback-Leiber distance is always non-negative. It equals to zero if and only if both comparable distributions are identical. In our case it implies that $\Delta H(t)$ is always positive (i.e., we have just proved inequality (5.95)), because tagged particle densities $\tilde{p}_{\mathrm{L}}(x;t)$, $\tilde{p}_{\mathrm{R}}(x;t)$ always differ from the single-particle density $\tilde{u}(x;t)$.

Moreover, the Kullback-Leiber distance $K[p,q]$ may be interpreted as a measure of the inefficiency of assuming that the distribution is q when true distribution is p [56]. Hence the quantity $\Delta H(t)/k_{\mathrm{B}}$ may serve as a measure of information neglected if we would try to approximate the tagged-particle densities $\tilde{p}_{\mathrm{L}}(x;t)$, $\tilde{p}_{\mathrm{R}}(x;t)$ by the single-particle density $\tilde{u}(x;t)$.

Chapter 6

Summary and outlook

In the thesis we have focused on the one dimensional diffusion of hard-core interacting particles diffusing in the external time-dependent forcefield. Our approach was based on the general Theorem 4.1 stated about the form solution of the underlying Smoluchowski equation. This theorem enables us to construct the probability density of particle's coordinates for N interacting particles as the properly symmetrized product of the simpler elements. Namely, of the probability density of the single diffusing particle. Up to our knowledge, this theorem is not yet presented in the scientific literature and all known exact analytical results could be derived as the particular cases of this theorem.

As the particular example, we have studied in detail the diffusion of two hard-core interacting particles on the half-line with an reflecting boundary placed at the origin of coordinates. Particles were under the action of the time-oscillating force superimposed on the time-independent force. The most interesting physics occurs when the latter force permanently pushes particles against the reflecting boundary. We have implemented two approaches to obtain probability densities of particle's positions. Firstly, we have used the numerical approach to study the transient dynamics. Secondly, we have derived the exact analytical expressions for the probability densities in the time-asymptotic regime. This exact analytical approach formed the basis for studying the dynamics of mean positions and thermodynamic characteristics.

One of our aims was to explore the influence of the interaction on the kinetics and energetics of the individual particles. It was demonstrated that the hard-core interaction restricts the motion of individual particles. It introduces the effective repulsive interaction between the particles. Hence it changes the quantitative features of the dynamics and energetics of the individual particles. Up to one exception, all averaged quantities (mean positions, internal energies, work, heat, entropy productions) behave qualitatively in the same manner. They seems to be only differently scaled for individual

particles. Moreover, overall values of these averaged quantities e.g. of internal energies, exhibit one common feature. The sum of the internal energies of two interacting particles is equal to the sum of the internal energies of two non-interacting particles. This holds also for mean positions, work, heat and the total entropy production. The only exception is the entropy. The sum of the instantaneous entropies of individual interacting particles is always smaller for than the entropy of the whole system. In the case without interaction these two entropies are equal.

The main features of the energetics are common for both the system with two interacting particles and the system consisted of non-interacting particles. In the stationary regime, the system exhibits periodic changes of its state. Therefore its internal energy, as every state function is also periodic. This of course says nothing about the period-averaged value of the internal energy. This time-averaged energy content in the stationary non-equilibrium regime, when heat is being released at fixed bath-temperature, is always higher than the equilibrium internal energy corresponding to the same temperature. Having periodic changes of the internal energy, the work done on the system during one period must be equal to the heat dissipated during the period. However, their behaviour during an infinitesimal time-interval within the period is quite different. Both heat and work could be positive or negative during this intervals, but on the whole, the work done on the system per one period is always positive. Hence the heat released to the reservoir per one period is also positive. This heat divided by the temperature of the heat bath forms the increase of the total entropy per one period (the entropy of the system is also a state function, hence it is periodic).

In spite of exact analytical results for the probability densities of positions, we also derived the analytical expressions for other important characteristics. As the basis for these derivations served the Fourier series representations of the mean positions. We derived the expressions for the internal energies as the functions of time, the averaged internal energies over the period (up to a multiplicative prefactor they are given by zero Fourier coefficients of the expansion of corresponding mean position), work, heat and entropy productions per one period. The three latter quantities are given by the first Fourier coefficients of the expansions of mean positions with a convenient multiplicative prefactors. This enables us to study characteristics per period as the functions of model parameters. Both works (heats) and entropy productions per period of individual particles exhibit maxima as the functions of the frequency. The entropy productions per period are symmetric under the change of heat bath temperature and the frequency of the driving force. This symmetry is more surprising (as discussed in Sec. 5.2.4) due to the completely different physical background of the influence of these quantities on the entropy production.

Although we have closely examined only the case of two interacting particles, the

qualitative results are valid in general. The extension to more particles is straightforward and does not introduce any new qualitative unexpected effects into the problem. However, there are many other perspectives to the future study of the model and much more possible extensions.

Future research can goes beyond the mean values of thermodynamics characteristics. We can try to derive the probability density of work or heat within the period and test the fluctuation theorems in the presence of interaction among the particles. Other direction of future research can consist in superimposing of attractive or repulsive interactions on the hard-core interaction among the particles or in obtaining the hard-core interaction as a limit of finite interacting potential[1]. Also it can be very interesting to go beyond the over-damped approximation, i.e., to try to formulate and solve the *Kramers equation* instead of the Smoluchowski equation and to investigate the behaviour of velocities of the particles. This will certainly enrich th kinetic and thermodynamic characteristics. On the other hand the diffusion of Brownian particles could be regarded as the limit of a random walk in continuous time. Probabilities in such a models are governed by the master equation. Hence we can formulate the master equation, which gives in the limit the Smoluchowski equation. Then we could try to construct the solution of the master equation in a similar manner as in the continuous case. Thus that seems to be possible to obtain the exactly solvable externally driven TASEP-like model.

Also we believe that this purely theoretical study will contribute to better understanding of non-equilibrium phenomena in experimentally relevant systems. Concretely in the systems in which the diffusion phenomena is taking place in the confined geometry and with the presence of driving forces.

[1] As was done for two particles without external driving in [41].

Bibliography

[1] Derrida B., Domany E., Mukamel D.: *An exact solution of the one dimensional asymmetric exclusion model with open boundaries*, J. Stat. Phys. **69** (1992) 667.

[2] Derrida B., Evans M. R., Hakim V., Pasquier V.: *Exact solution of a 1d asymmetric exclusion model using a matrix formulation*, J. Phys. A **26** (1993) 1493.

[3] MacDonald J. T., Gibbs J. H., Pipkin A. C.: *Kinetics of biopolymerization on nucleic acid templates*, Biopolymers **6** (1968) 1.

[4] MacDonald J. T., Gibbs J. H.: *Concerning the kinetics of polypeptide synthesis on polyribosomes*, Biopolymers **7** (1969) 707.

[5] Basu A., Chowdhury D.: *Modeling protein synthesis from a physicist's perspective: a toy model*, Am. J. Phys **75** (2007) 931.

[6] Hill T. L., Chen Y.-D.: *Cooperative effects in models of steady-state transport across membranes IV. One-site, two-site, and multi-site models*, Biophys. J. **11** (1971) 685.

[7] Nagatani T.: *Creation and annihilation of traffic jams in a stochastic asymmetric exclusion model with open boundaries: a computer simulation*, J. Phys. A **28** (1995) 7079.

[8] Chowdhury D., Santen L., Schadschneider A.: *Statistical physics of vehicular traffic and some related systems*, Phys. Rep. **329** (2000) 199.

[9] Schadschneider A.: *Statistical mechanics of traffic flow*, Physica A **285** (2000) 101.

[10] Schütz G. M.: *Single-file diffusion far from equilibrium*, Diffusion Fundamentals **2** (2005) 5.1.

[11] Evans M. R., Sugden K. E. P.: *An exclusion process for modelling fungal hyphal growth*, Physica A **384** (2007) 53.

[12] Aghababaie Y., Menon G. I., Plischke M.: *Universal properties of interacting Brownian motors* Phys. Rev. E **59** (1999) 2578.

[13] Chou T., Lohse D.: *Entropy-driven pumping in zeolites and biological channels*, Phys. Rev. Lett. **82** (1999) 3552.

[14] Klumpp S., Lipowsky R.: *Traffic of Molecular Motors Through Tube-Like Compartments*, J. Stat. Phys. **113** (2003) 233.

[15] Lakatos G. W.: *Transport and structure in nanoscale channels*, PhD thesis, University of British Columbia, 2006.

[16] Kardar M., Parisi G., Zhang Y.-C.: *Dynamic scaling of growing interfaces*, Phys. Rev. Lett. **56** (1986) 889.

[17] Spitzer F.: *Interaction of Markov processes*, Adv. in Math. **5** (1970) 246.

[18] Blythe R. A., Evans M. R.: *Nonequilibrium steady states of matrix-product form: a solver's guide*, J. Phys. A **40** (2007) R333.

[19] Schütz G. M.: *Exact solution of the master equation for the asymmetric exclusion process*, J. Stat. Phys. **88** (1997) 427.

[20] Hodgkin A. L., Keynes R. D.: *The potassium permeability of giant nerve fibre*, J. Physiol. **128** (1955) 61.

[21] Schuring D.: *Diffusion in zeolites : towards a microscopic understanding*, PhD thesis, University Eindhoven, 2002.

[22] Hahn K., Kärger J., Kukla V.: *Single-file diffusion observation*, Phys. Rev. Lett. **76** (1996) 2762.

[23] Kärger J., Ruthven M.: *Diffusion in Zeolites and in Other Microporous Solids*, Wiley, New York, 1992.

[24] Dekker C.: *Solid-state nanopores*, Nat. Nanotechnol. **2** (2007) 209.

[25] Halpin-Healy T., Zhang Y.-C.: *Kinetic roughening phenomena, stochastic growth, directed polymers and all that. Aspects of multidisciplinary statistical mechanics*, Phys. Rep. **254** (1995) 215.

[26] Wei Q.-H., Bechinger C., Leiderer P.: *Single-file diffusion of colloids in one-dimensional channels*, Science **287** (2000) 625.

[27] Bechinger C.: *Diffusion in Reduced Dimensions* (presentation available on-line), Universität Stuttgart, 2. Physikalisches Institut, October 2008, Available at: <http://www.pi2.uni-stuttgart.de/contact/index.php?article_id=21>

[28] Lutz C., Kollmann M., Bechinger C.: *Single-file diffusion of colloids in one-dimensional channels*, Phys. Rev. Lett. **93** (2004) 026001.

[29] Chou C.-Y., Eng B. C., Robert M.: *One-dimensional diffusion of colloids in polymer solutions*, J. Chem. Phys. **124** (2006) 044902.

[30] Mukherjee B., Maiti P. K., Dasgupta C., Sood A. K.: *Structure and dynamics of confined water inside narrow carbon nanotubes*, Nanosci. Nanotechnol. **7** (2007) 1796.

[31] Cheng C.-Y., Bowers C. R.: *Observation of single-file diffusion in dipeptide nanotubes by continuous-flow hyperpolarized xenon-129 NMR spectroscopy*, Chem. Phys. Chem. **8** (2007) 2077.

[32] Van Gool W. in *Fast ion transport in solids*, edited by Van Gool W., North-Holland, Amsterdam, 1973, pp. 201-215.

[33] Harris T. E.: *Diffusion with "collisions" between particles*, J. Appl. Prob. **2** (1965) 323.

[34] Rödenbeck Ch., Kärger J., Hahn K.: *Calculating exact propagators in single-file systems via the reflection principle*, Phys. Rev. E **57** (1998) 4382.

[35] Kutner R.: *Chemical diffusion in the lattice gas of non-interacting particles*, Phys. Lett. A **81** (1981) 239.

[36] Van Beijeren H., Kehr K. W., Kutner R.: *Diffusion in concentrated lattice gases. III. Tracer diffusion on a one-dimensional lattice*, Phys. Rev. B **28** (1983) 5711.

[37] Lizana L., Ambjörnsson T.: *Diffusion of finite-sized hard-core interacting particles in a one-dimensional box: Tagged particle dynamics*, Phys. Rev. E **80** (2009) 051103.

[38] Kumar D.: *Diffusion of interacting particles in one dimension*, Phys. Rev. E **78** (2008) 021133.

[39] Batchelor M. T.: *The Bethe ansatz after 75 years*, Phys. Today **60** (2007) 36.

[40] Ambjörnsson T., Lizana L., Lomholt M. A., Silbey R. J.: *Single-file dynamics with different diffusion constants*, J. Chem. Phys. **129** (2008) 185106.

[41] Ambjörnsson T., Silbey R. J.: *Diffusion of two particles with a finite interaction potential in one dimension*, J. Chem. Phys. **129** (2008) 165103.

[42] Ambjörnsson T., Silbey R. J.: *Theory of single file diffusion in a force field*, Phys. Rev. Lett. **102** (2009) 050602.

[43] Barkai E., Silbey R. J.: *Diffusion of tagged particle in an exclusion process*, arXiv:1001.0732v1 [cond-mat.stat-mech] (2010).

[44] Karlin S., and McGregor J.: *Coincidence probabilities*, Pacific J. Math. **9** (1959) 1141.

[45] Massey, W. A.: *Calculating exit times for series Jackson networks*, J. Appl. Prob. **24** (1987) 226.

[46] Baccelli F., Massey W.A.: *A Transient Analysis of the Two-Node Series Jackson Network*, Rapport INRIA No. 852 (1988)

[47] Dieker, A. B., Warren, J.: *Determinantal transition kernels for some interacting particles on the line* Ann. Inst. H. Poincaré Probab. Statist. **44** (2008) 1162.

[48] Dieker, A. B., Warren, J.: *Series Jackson Networks and Noncrossing Probabilities* Math. Op. Res., published online before print December 8, 2009.

[49] Böhm W., Jain J. L., Mohanty S. G.: *On zero avoiding transition probabilities of an r-node tandem queue: a combinatorial approach*, J. Appl. Prob. **30** (1993) 737.

[50] Fisher M. E.: *Walks, walls, wetting, and melting* J. Stat. Phys. **34** (1984) 667.

[51] Risken H.: *The Fokker-Planck Equation: Methods of Solutions and Applications*, Springer-Verlag, Berlin, 1989.

[52] Van Kampen N. G.: *Stochastic Process in Physics and Chemistry*, Elsevier, New York, 2007.

[53] Gardiner C. W.: *Handbook of Stochastic Methods: for Physics, Chemistry and the Natural Sciences (Springer Series in Synergetics)*, Springer, Berlin, 1997.

[54] Sekimoto K.: *Kinetic characterization of heat bath and the energetics of thermal ratchet models*, J. Phys. Soc. Jpn. **66** (1997) 1234.

[55] Kullback S., Leibler R. A.: *On Information and Sufficiency*, Ann. Math. Stat. **22** (1951) 79.

[56] Cover T. M., Thomas J. A.: *Elements of information theory*, John Wiley & Sons, Inc., New York, 1991.

[57] Papoulis A.: *Probability, random variables, and stochastic processes*, McGraw-Hill, Inc., New York, 1991.

[58] Chvosta P., Schulz M., Paule E., Reineker P.: *Kinetics and energetics of reflected diffusion process with time-dependent and space-homogeneous force*, New. J. Phys. **7** (2005) 190.

[59] Chvosta P., Schulz M., Mayr E., Reineker P.: *Sedimentation of particles acted upon by a vertical time-oscillating force*, New. J. Phys. **7** (2005) 190.

[60] Hänggi P., Thomas H.: *Linear response and fluctuation theorems for nonstationary stochastic processes*, Z. Physik B **22** (1975) 295.

[61] Hänggi P., Thomas H.: *Time evolution, correlations, and linear response of non-Markov processes*, Z. Physik B **26** (1977) 85.

[62] Wolf F.: *Lie algebraic solutions of linear Fokker-Planck equations*, J. Math. Phys. **29** (1988) 305.

[63] Doetsch G.: *Anleitung zum praktischen Gebrauch der Laplace-Transformation und der Z-Transformation* München: R. Oldenbourg, 1967.

[64] Abramowitz M., Stegun I. A. (editors): *Handbook of Mathematical Functions* National Bureau of Standards, New York, Dover, 1970.

[65] Aslangul C.: *Diffusion of two repulsive particles in a one-dimensional lattice*, J. Phys. A: Math. Gen. **32** (1999) 3993.

[66] Rief F.: *Fundamentals of statistical and thermal physics*, McGraw-Hill, Inc., New York, 1965.

[67] Weiss R., Anderssen R. S.: *A product integration method for a class of singular first kind Volterra equations*, Numer. Math. **18** (1972) 442.